STUDIES ON THE CHEMISTRY, ANTICHOLINESTERASE ACTIVITY AND TOXICITY OF *Mitragyna speciosa* (KRATOM) ALKALOIDS

NELSON CHEAR JENG YEOU

UNIVERSITI SAINS MALAYSIA

2024

STUDIES ON THE CHEMISTRY, ANTICHOLINESTERASE ACTIVITY AND TOXICITY OF *Mitragyna speciosa* (KRATOM) ALKALOIDS

by

NELSON CHEAR JENG YEOU

Thesis submitted in fulfilment of the requirements
for the degree of
Doctor of Philosophy

June 2024

ACKNOWLEDGEMENT

First and foremost, I would like to express my gratitude to God for giving me the opportunity and helping me endlessly finish the PhD study entitled 'Studies on the chemistry, anticholinesterase activity and toxicity of *Mitragyna speciosa* (Kratom) alkaloids'. Secondly, I would like to express my deepest gratitude to my supervisor, Professor Dr Surash Ramanathan, for giving me his guidance and continuous encouragement throughout my PhD journey. He always does his best to give me the maximum support and freedom in designing the experiment, conception of research ideas, writing grant proposals, writing research articles, etc. I would also like to extend my gratitude to my co-supervisor, Professor Dr Vikneswaran Murugaiyah, for his help, advice, and moral support in going through the many hiccups that I faced throughout my studies. Thirdly, I would like to thank my field supervisor, Prof. Dr Christopher R. McCurdy, for providing me with the chance to conduct research training in the area of natural products chemistry, analytical chemistry, and opioid pharmacology at the University of Florida (UF) under the United States Exchange Visitor Programme.

Special thanks to my chemistry mentor, Dr Juan Francisco León (formerly affiliated with the University of Florida), for his help and guidance until the final stage of this research project, particularly in alkaloid isolation and NMR structure elucidation. I want to thank James Rocca, a well-experienced NMR specialist at the University of Florida, for his help and guidance in handling NMR instruments and spectral acquisition.

On top of these, I would like to acknowledge the Research Creativity and Management Office (RCMO) and Institute of Postgraduate Studies, Universiti Sains Malaysia (USM), for their financial support in the completion of this thesis under the

Research University Grant and USM Fellowship Scheme, respectively. I also thank the Centre for Drug Research (USM) and College of Pharmacy (UF) for providing me with the research equipment, facilities, and a conducive environment to conduct the experiments.

I have been fortunate enough to have many people who have helped or assisted me in this journey. I could not have completed my research project smoothly without their continuous support and assistance. Special thanks to Mr Hilman for their service in acquiring GC-MS data. I also thank Mr Asokan, Mr Hilman, Mr Rahim and other lab and administrative staff who have helped me in one way or another. Many thanks to my colleagues, lab mates, and research collaborators, Dr Siti, Dr Juzaili, Dr Darshan, and Assoc. Prof. Dr Zurina, Dr Farah, Dr Tan, Dr Khaw, Puan Sabrina, Anuar, Ai Fein, Boon Keat, Waleed, Azlan, etc., for lending their hands or moral support during my hard time. I greatly appreciated it.

Finally, I thank my dearest mom and dad and my sister Alice for all their encouragement, understanding and sacrifices made throughout these years to complete my PhD study smoothly.

TABLE OF CONTENTS

ACKNOWLEDGEMENT ..... **ii**

TABLE OF CONTENTS ..... **iv**

LIST OF TABLES ..... **x**

LIST OF FIGURES ..... **xii**

LIST OF SYMBOLS AND ABBREVIATIONS ..... **xxiii**

ABSTRAK ..... **xxvi**

ABSTRACT ..... **xxviii**

CHAPTER 1 INTRODUCTION **1**

1.1 Overview 1

1.2 Problem statement 4

1.3 Research objectives 6

1.4 Experiment design 7

CHAPTER 2 LITERATURE REVIEW **8**

2.1 Alzheimer's disease (AD) 8

2.2 Neuropathological hallmarks of AD 9

2.2.1 Amyloid hypothesis 11

2.2.2 Tau hypothesis 11

2.2.2 Cholinergic hypothesis 12

2.3 Cholinesterase enzyme 13

2.4 Current treatment for AD 17

2.5 Plant alkaloids as lead compounds for treating CNS diseases 18

2.5.1 Classification of alkaloids 22

2.5.1(a) Biochemical origin 22

2.5.1(b) Chemical strucutre 23

2.5.1(c) Taxonimical origin 24

2.5.1(d) Pharmacological action 25
2.5.2 Plant alkaloids as a source of cholinesterase inhibitors 25
2.5.2(a) Quinolizidine-type alkaloids from Lycopodiacea 28
2.5.2(b) Isoquinoline alkaloids from Amaryllidaceae 30
2.5.2(c) Indole *β*-carbolines from Nitrariaceae 33
2.6 Rubiaceae family 35
2.6.1 Rubiaceous alkaloids as a source of cholinesterase inhibitors..... 37
2.6.1(a) Cholinesterase inhibitors from *Psychotria* genus 39
2.6.1(b) Cholinesterase inhibitors from *Nauclea* genus..... 40
2.6.1(c) Cholinesterase inhibitors from *Uncaria* genus 42
2.7 *Mitragyna speciosa* (Korth) Havil. 44
2.7.1 Botanical description and geographical distribution……...45
2.7.2 Traditional uses…….. 47
2.7.3 Phytochemistry…….. 48
2.7.3(a) Monoterpene indole alkaloids…….. 49
2.7.3(b) Monoterpene oxindole alkaloids…….. .54
2.7.4 CNS pharmacological targets of *M. speciosa* alkaloids……..57
2.7.4(a) Opioid receptors……... .57
2.7.4(b) Serotonin receptors……... .59
2.7.4(c) Adrenergic receptors…… .61
2.7.4(d) Cholinesterase enzyme……. .63
CHAPTER 3 METHODOLOGY..... 64
3.1 Research materials 64
3.1.1 Chemicals..... ….64
3.1.2 Equipment and instrumentation 66
3.2 Plant material 66
3.3 Experimental methods..... 68

3.3.1 Small-scale extraction of plant materials ..... ….68

3.3.1(a) Maceration…..……...68

3.3.1(b) Hot maceration 68

3.3.1(c) Ultrasound-assisted extraction..... 69

3.3.1(d) Soxhlet extraction..... 69

3.3.2 Large-scale extraction of plant material..... 69

3.3.3 Acid-base extraction 70

3.3.4 Chromatography 71

3.3.4(a) Fractionation of the alkaloid extract 71

3.3.4(b) Isolation of (**87**) and (**101**) from fraction F2 72

3.3.4(b)(i) Compound (**87**)..... 72

3.3.4(b)(ii) Compound (**101**)……..……..72

3.3.4(c) Isolation of (**81**), (**89**) and (**91**) from fraction F3..... 73

3.3.4(c)(i) Compound (**91**)…….……...74

3.3.4(c)(ii) Compound (**81**)……74

3.3.4(c)(iii) Compound (**89**)……74

3.3.4(d) Isolation of (**82**) and (**125**) from fraction F4…….75

3.3.4(d)(i) Compound (**125**)……..76

3.3.4(d)(ii) Compound (**82**)……76

3.3.4(e) Isolation of (**88**) and (**117**) from fraction F5.....76

3.3.4(e)(i) Compound (**117**)…..…..……...77

3.3.4(e)(ii) Compound (**88**)……77

3.3.4(f) Isolation of (**90**), (**98**), (**146**) and (**116**) from fraction F6.....78

3.3.4(f)(i) Compound (**90**)…….……...78

3.3.4(f)(ii) Compound (**146**)……..79

3.3.4(f)(iii) Compound (**98**)……80

3.3.4(f)(iv) Compound (**116**)……..……80

3.3.5 Compound identification and structure elucidation 80
3.3.5(a) Gas chromatography-mass spectrometry …..……...80
3.3.5(b) High resolution-mass spectrometry.....…..…….....81
3.3.5(c) Ultraviolet-visible (UV-VIS) spectroscopy …..…....81
3.3.5(d) Fourier Transformed Infrared Spectroscopy..... 82
3.3.5(e) Nuclear magnetic resonance spectroscopy.....82
3.3.5(f) Electron circular dichroism (ECD) spectroscopy.....83
3.3.5(g) Melting point analyzer.....83
3.3.6 Bioassays..... ….83
3.3.6(a) *In vitro* anticholinesterase activity……..... 83
3.3.6(b) Enzyme kinetics and mode of inhibition…….. 84
3.3.6(c) Cytotoxicity..... ……..... 85
3.3.6(c)(i) Cell culture and maintenance……...85
3.3.6(c)(ii) MTT assay.....…….. 85
3.3.6(d) Opioid receptors radioligand binding assay.....86
3.3.7 Molecular docking studies ..... ….87
3.3.8 Data analysis ..... ….88
3.4 Isolation scheme of *M. speciosa* alkaloids 89
CHAPTER 4 RESULTS AND DISCUSSION 90
4.1 General 90
4.2 Comparison of different extraction methods..... 90
4.3 *In vitro* anticholinesterase activity of the methanol and alkaloid extracts 93
4.4 Bioassay-guided fractionation of compounds from the alkaloid extract..... .96
4.4.1 Anticholinesterase activity of fractions F1-F7..... 96
4.5 Isolation of bioactive alkaloids from the active fractions F2-F6 98
4.6 Identification of alkaloid constituents from the active fractions F2-F6.....100
4.6.1 Identification of compounds (**87**) and (**101**) in fraction F2.....100

4.6.1(a) Compound (**87**)…….....101

4.6.1(b) Compound (**101**).....122

4.6.2 Identification of compounds (**81**), (**89**) and (**91**) in fraction F3.....140

4.6.2(a) Compound (**89**)……..... 141

4.6.2(b) Compound (**91**)…..……..... 158

4.6.2(c) Compound (**81**)...…….....176

4.6.3 Identification of compounds (**82**) and (**125**) in fraction F4.....193

4.6.3(a) Compound (**82**)…….....194

4.6.3(b) Compound (**125**)…….....215

4.6.4 Identification of compounds (**117**) and (**88**) in fraction F5..... 233

4.6.4(a) Compound (**117**)…….....234

4.6.4(b) Compound (**88**)...…….....255

4.6.5 Identification of compounds (**90**), (**146**), (**98**) and (**116**) in fraction F6..... 274

4.6.5(a) Compound (**90**)…….....277

4.6.5(b) Compound (**146**)…..…….….....295

4.6.5(c) Compound (**98**)...…….…….....313

4.6.5(d) Compound (**116**)...…….…….....333

4.6.6 Analysis of the isolated alkaloids using TLC and GC-MS 353

4.7 Anticholinesterase activity of the isolated alkaloids..... 368

4.7.1 Structure-inhibition relationships of the isolated alkaloids towards AChE and BChE enzymes..... 376

4.7.2 Kinetic studies of the most active alkaloids (**81**) and **(89**).....386

4.7.3 Molecular docking studies of compounds (**81**), **(91**) and (**89**)..... 388

4.8 Opioid-receptors binding affinity of isolated alkaloids from *M. speciosa*... 393

4.9 Cytotoxicity of the isolated alkaloids from *M. speciosa*..... 400

CHAPTER 5 CONCLUSION..... 404

REFERENCES 408

LIST OF PUBLICATIONS

LIST OF TABLES

Page

Table 2.1 Privileged alkaloid scaffolds among CNS drugs…….....…..19

Table 3.1 Solvent gradient used for fractionation of the alkaloid extract….....71

Table 3.2 Solvent gradient used for isolation of (**81**), (**89**) and (**91**).…….…….……..73

Table 3.3 Solvent gradient used for isolation of compounds (**125**) and (**82**)…...75

Table 3.4 Solvent gradient used for isolation of compounds (**88**) and (**117**)…...76

Table 3.5 Solvent gradient used for fractionation of compounds (**90**), (**98**), (**146**), and (**116**).....……...…….. .78

Table 3.6 Solvent gradient used for isolation of compounds (**90**) and (**146**).....……..……...……....79

Table 4.1 Cholinesterase inhibitory activity of *M. speciosa* extracts..... 94

Table 4.2 Cholinesterase inhibitory activity of the combined fractions, F1-F7.....97

Table 4.3 ^{1}H and ^{13}C NMR data of compound (**87**).....111

Table 4.4 ^{1}H and ^{13}C NMR data of compound (**101**).....127

Table 4.5 ^{1}H and ^{13}C NMR data of compound (**89**).....146

Table 4.6 ^{1}H and ^{13}C NMR data of compound (**91**).....165

Table 4.7 ^{1}H and ^{13}C NMR data of compound (**81**).....183

Table 4.8 ^{1}H and ^{13}C NMR data of compound (**82**).....199

Table 4.9 ^{1}H and ^{13}C NMR data of compound (**125**).....220

Table 4.10 ^{1}H and ^{13}C NMR data of compound (**117**).....241

Table 4.11 ^{1}H and ^{13}C NMR data of compound (**88**).....262

Table 4.12 ^{1}H and ^{13}C NMR data of compound (**90**).....282

Table 4.13 ^{1}H and ^{13}C NMR data of compound (**146**).....298

Table 4.14 ^{1}H and ^{13}C NMR data of compound (**98**).....316

Table 4.15 ^{1}H and ^{13}C NMR data of compound (**116**).....339

Table 4.16 Anticholinesterase activity of major *M. speciosa* alkaloids from the active fractions F2-F6.....374

Table 4.17 List of the alkaloids present in the active fractions F2-F6 and their corresponding anticholinesterase activity.....375

Table 4.18 Kinetic parameters of AChE and BChE in the presence of the active alkaloids (**81**) and (**89**), respectively.....388

Table 4.19 Binding interaction data for compounds (**91**), (**89**) and (**81**) docked into active site gorge of *Tc*AChE and *h*BChE.....388

Table 4.20 Percent displacement of radioligands by selected *M. speciosa* alkaloids at opioid receptor subtypes in a screening profile.....392

Table 4.21 *Ki* values of selected *M. speciosa* alkaloids at the human μ-opioid receptors.....398

Table 4.22 Cytotoxicity of *M. speciosa* alkaloids on selected cell lines.....400

LIST OF FIGURES

Page

Figure 1.1 Flow chart of the designed study……..…….7

Figure 2.1 The brain region of a healthy person and AD patient…...……...10

Figure 2.2 The reaction step of the hydrolysis of acetylcholine (**1**) by cholinesterase……..……...…14

Figure 2.3 Protein structure of (**a**) acetylcholinesterase (AChE); (**b**) butyrylcholinesterase (BChE)…...……..…….....16

Figure 2.4 Mechanism of action of central AChE and BChE inhibitors according to the cholinergic hypothesis ……..……...16

Figure 2.5 Structural similarity between neurotransmitters and alkaloid-derived CNS drugs…….……..……..24

Figure 2.6 Structural classes of alkaloids based on their ring structure …….……..……..26

Figure 2.7 Alkaloidal backbone of donepezil (7), rivastigmine (8), galantamine (9) and physostigmine (26)..…….……..28

Figure 2.8 Structural classes of lycopodium alkaloids ……...…….31

Figure 2.9 Representative chemical structure for the main groups of Amaryllidaceae alkaloids……...……..……...33

Figure 2.10 Subfamilies and tribes under the Rubiaceae family……..……38

Figure 2.11 Biosynthesis pathway of corynanthe-, iboga- and aspidosperma-type alkaloids……...…..…… 40

Figure 2.12 The pictures of (**a**) *M. speciosa* trees; (**b**) cluster of *M. speciosa* flowers; (**c**) *M. speciosa* fruits; (**d**) green and red veins of *M. speciosa* leaves.……...…….. 48

Figure 2.13 Distribution map of *M. speciosa* in Southeast Asia (green colour)……...……49

Figure 2.14 Preparation of decoction from the fresh leaves of *M. speciosa*..……..……..……50

Figure 2.15 Important structural features of mitragynine (**87**)……..……52

Figure 3.1 Voucher specimen of *Mitragyna speciosa*……..…..……..……69

Figure 3.2 Isolation scheme of alkaloid constituents from the leaves of *M. speciosa*……..……..…..…..……90

Figure 4.1 Extraction yields (average of $n = 3$) of *M. speciosa* methanol extracts obtained using various extraction methods.……..……92

Figure 4.2 Extraction yields (average of $n = 3$) of *M. speciosa* alkaloid extracts obtained using various extraction methods.……..…..……93

Figure 4.3 Dose-dependent curve (mean ± SD; $n = 3 \times 2$) of methanol and alkaloid extracts against (**A**) AChE and (**B**) BChE.....……96

Figure 4.4 Percentage yield of the combined fractions (F1 - F7) obtained from the alkaloid extract.....……97

Figure 4.5 TLC profiles of (**A**) F2 to F6, developed by DCM: EtOAc (7:3, *v/v*) and viewed under UV-365nm, and (**B**) F5 and F6, developed by $CHCl_3$: MeOH (9.5: 0.5, *v/v*) and viewed under UV-365nm. The arrow indicated the detected compounds.....…….……...100

Figure 4.6 GC-MS chromatogram of fraction F2……...……..101

Figure 4.7 (**A**) GC-MS chromatogram, (**B**) EI-MS spectrum and (**C**) major EI-MS fragments of compound (**87**)…….…..…….…… 104

Figure 4.8 (**A**) Scheme I – Fragments **87a**, **87b**, **87c** and **87d**; (**B**) Scheme II – fragments **87e** and **87f**; (**C**) Scheme III – fragments **87g**, **87h**, and **87i**; and (**D**) Scheme IV – fragment **87j**……..…….....108

Figure 4.9 UV spectrum of compound (**87**) in methanol……..……..108

Figure 4.10 IR spectrum of compound (**87**) (KBr)……..……..……..109

Figure 4.11 ^{1}H NMR spectrum of compound (**87**) ($CDCl_3$, 500 MHz)...…...114

Figure 4.12 ^{13}C NMR spectrum of compound (**87**) ($CDCl_3$, 125 MHz).....115

Figure 4.13 **(A**) DEPT 135 and (**B**) DEPT 90 spectra of compound (**87**).....116

Figure 4.14 HSQC spectrum of compound (**87).……..**117

Figure 4.15 (**A**) HMBC spectrum, (**B**) Enlarged HMBC spectrum – Part I, (**C**) Enlarged HMBC spectrum – Part II, (**D**) Enlarged HMBC spectrum – Part III and (**E**) Enlarged HMBC spectrum – Part IV of compound (**87**).....120

Figure 4.16 Selected HMBC correlations of compound (**87**)……..120

Figure 4.17 (**A**) COSY spectrum, (**B**) Enlarged COSY spectrum – Part I and (**C**) Enlarged COSY spectrum – Part II of compound (**87**)……122
Figure 4.18 Proposed structure of compound (**87**)……..123

Figure 4.19 (**A**) GC-MS chromatogram and (**B**) EI-MS spectrum of compound (**101**)…….125

Figure 4.20 UV spectrum of compound (**101**) in methanol.....124

Figure 4.21 ^{13}C NMR spectrum of compound (**101**) ($CDCl_3$, 125 MHz).....130

Figure 4.22 (**A**) DEPT 90 and (**B**) DEPT 135 spectra of compound (**101**).....131

Figure 4.23 ^{1}H NMR spectrum of compound (**101**) ($CDCl_3$, 500 MHz)…….132

Figure 4.24 (**A**) Full HSQC spectrum; (**B**) Enlarged HSQC spectrum – Part I; and (**C**) Enlarged HSQC spectrum – Part II of compound (**101**)..134

Figure 4.25 (**A**) COSY spectrum; (**B**) Enlarged COSY spectrum – Part I; (**C**) Enlarged COSY spectrum – Part II of compound (**101**)……136

Figure 4.26 (**A**) Full HMBC spectrum; (**B**) Enlarged HMBC spectrum – Part I; (**C**) Enlarged HMBC spectrum - Part II; (**D**) Enlarged HMBC spectrum – Part III and (**E**) Enlarged HMBC spectrum – Part IV of compound (**101**)……..……140

Figure 4.27 Selected COSY and HMBC correlation of compound (**101**)……140

Figure 4.28 Proposed structure of compound (**101**)…….141

Figure 4.29 GC-MS chromatogram of fraction F3.....141

Figure 4.30 (**A**) GC-MS chromatogram and (**B**) EI-MS spectrum of compound (**89**)……...143

Figure 4.31 UV spectrum of compound (**89**) in methanol.....144

Figure 4.32 IR spectrum of compound (**89**) (KBr)……...145

Figure 4.33 ^{13}C NMR spectrum of compound (**89**) ($CDCl_3$, 125 MHz).....149

Figure 4.34 (**A**) DEPT 135 and (**B**) DEPT 90 spectra of compound (**89**).....150

Figure 4.35 ^{1}H NMR spectrum of compound (**89**) ($CDCl_3$, 500 MHz).....151

Figure 4.36 (**A**) HMBC spectrum, (**B**) Enlarged HMBC spectrum – Part I, (**C**) Enlarged HMBC spectrum – Part II; and (**D**) Enlarged HMBC spectrum – Part III of compound (**89**)……..152

Figure 4.37 HSQC spectrum of compound (**89**)…....……..155

Figure 4.38 (**A**) Full COSY spectrum, (**B**) Enlarged COSY spectrum – Part I, and (**C**) Enlarged COSY spectrum – Part II of compound (**89**)...158

Figure 4.39 Selected COSY and HMBC correlations of compound (**89**).....154

Figure 4.40 Proposed structure of compound (**89**).....158

Figure 4.41 HR-ESI-MS (positive mode) spectrum of compound (**91**)……..160

Figure 4.42 UV spectrum of compound (**91**) in methanol……...159

Figure 4.43 IR spectrum of compound (**91**) (KBr).....161

Figure 4.44 (**A**) GC-MS chromatogram and (**B**) EI-MS spectrum of compound (**91**).....163

Figure 4.45 ^{13}C NMR spectrum of compound (**91**) ($CDCl_3$, 125 MHz).....168

Figure 4.46 (**A**) DEPT 135 and (**B**) DEPT 90 spectra of compound (**91**)……169

Figure 4.47 ^{1}H NMR spectrum of compound (**91**) ($CDCl_3$, 500 MHz)……...170

Figure 4.48 HMBC spectrum of compound (**91**) ……..…….. 171

Figure 4.49 Selected COSY and HMBC correlations of compound (**91**)……171

Figure 4.50 HSQC spectrum of compound (**91**).....172

Figure 4.51 (**A**) Full COSY spectrum, (**B**) Enlarged COSY spectrum – Part I, and (**C**) Enlarged COSY spectrum – Part II of compound (**91**)…174

Figure 4.52 NOESY spectrum of compound (**91**)……...175

Figure 4.53 Selected NOESY correlations of compound (**91**)…….176

Figure 4.54 Proposed structure of compound (**91**).....176

Figure 4.55 (**A**) GC-MS chromatogram and (**B**) EI-MS spectrum of compound (**81**).....178

Figure 4.56 EI-MS fragmentation pattern of compound (**81**)……..179

Figure 4.57 UV spectrum of compound (**81**) in methanol……180

Figure 4.58 IR spectrum of compound (**81**) (KBr)……...181

Figure 4.59 ^{13}C NMR spectrum of compound (**81**) ($CDCl_3$; 125 MHz)…….186

Figure 4.60 HSQC spectrum of compound (**81**)……..……...187

Figure 4.61 ^{1}H NMR spectrum of compound (**81**) ($CDCl_3$; 500 MHz)……..188

Figure 4.62 (**A**) Full HMBC spectrum, (**B**) Enlarged HMBC spectrum – Part I, and (**C**) Enlarged HMBC spectrum – Part II of compound (**81**)....190

Figure 4.63 (**A**) Full COSY spectrum, (**B**) Enlarged COSY spectrum – Part I, and (**C**) Enlarged COSY spectrum – Part II of compound (**81**)….192

Figure 4.64 Selected COSY and HMBC correlations of compound (**81**)……192

Figure 4.65 ECD spectrum of compound (**81**) (MeOH; 20 µg/mL)……193

Figure 4.66 Proposed chemical structure of compound **(81**)……...193

Figure 4.67 GC-MS chromatogram of fraction F4……..……194

Figure 4.68 HR-ESI-MS (positive mode) spectrum of compound (**82**)……...196

Figure 4.69 (**A**) GC-MS chromatogram and (**B**) EI-MS spectrum of compound (**82**)……...197

Figure 4.70 UV spectrum of compound (**82**) in methanol.....198

Figure 4.71 ^{1}H NMR spectrum of compound (**82**) (500 MHz; $CDCl_3$)……...202

Figure 4.72 ^{13}C NMR spectrum of compound (**82**) (125 MHz; $CDCl_3$)……..203

Figure 4.73 (**A**) DEPT 135 and (**B**) DEPT 90 spectra of compound (**82**)……204

Figure 4.74 (**A**) HSQC spectrum, (**B**) Enlarged HSQC spectrum – Part I, and (**C**) Enlarged HSQC spectrum – Part II of compound (**82**)……206

Figure 4.75 (**A**) COSY spectrum, (**B**) Enlarged COSY spectrum – Part I, and (**C**) Enlarged COSY spectrum – Part II of compound (**82**).....207

Figure 4.76 (**A**) HMBC spectrum, (**B**) Enlarged HMBC spectrum – Part I, (**C**) Enlarged HMBC spectrum – Part II, (**D**) Enlarged HMBC spectrum – Part III and (**E**) Enlarged HMBC spectrum – Part IV of compound (**82**).....211

Figure 4.77 Selected COSY and HMBC correlations of compound (**82**)……211

Figure 4.78 (**A**) NOESY spectrum; (**B**) Enlarged NOESY spectrum – Part I and (**C**) Enlarged NOESY spectrum – Part II of compound (**82**)……213

Figure 4.79 Two possible chemical conformations of compound (**82**): 7*S* or 7*R*, and their characteristic NOE correlations.....214

Figure 4.80 Selected NOESY correlations of compound (**82**)…….215

Figure 4.81 Proposed structure of compound (**82**)……...215

Figure 4.82 (**A**) GC-MS chromatogram and (**B**) EI-MS spectrum of compound (**125**)…….217

Figure 4.83 UV spectrum of compound (**125**) in methanol…….218

Figure 4.84 ^{1}H NMR spectrum of compound (**125**) (CD_3OD; 600 MHz)……223

Figure 4.85 ^{13}C NMR spectrum of compound (**125**) (CD_3OD, 150 MHz)…..224

Figure 4.86 (**A**) HSQC spectrum, (**B**) Enlarged HSQC spectrum – Part I, (**C**) Enlarged HSQC spectrum – Part II, and (**D**) Enlarged HSQC spectrum – Part III of compound (**125**)…….…226

Figure 4.87 (**A**) COSY spectrum, (**B**) Enlarged COSY spectrum – Part I, and (**C**) Enlarged COSY spectrum – Part II of compound (**125**)……...228

Figure 4.88 (**A**) HMBC spectrum, (**B**) Enlarged HMBC spectrum – Part I, (**C**) Enlarged HMBC spectrum – Part II, (**D**) Enlarged HMBC spectrum – Part III, and (**E**) Enlarged HMBC spectrum – Part IV of compound (**125**).....231

Figure 4.89 Selected HMBC correlations of compound (**125**)……231

Figure 4.90 NOESY spectrum of compound (**125**).....232

Figure 4.91 Selected NOESY correlations of compound (**125**)……...233

Figure 4.92 ECD spectrum of compound (**125**) (MeOH, 20 µg/mL)…….…..233

Figure 4.93 Proposed structure of mitrafoline (**125**)……234

Figure 4.94 GC-MS chromatogram of fraction F5……. .235

Figure 4.95 HR-ESI-MS spectrum (positive mode) of compound (**117**)…….236

Figure 4.96 (**A**) GC-MS chromatogram and (**B**) EI-MS spectrum of compound (**117**)…….237

Figure 4.97 IR spectrum of compound (**117**) (KBr)……238

Figure 4.98 ^{1}H NMR spectrum of compound (**117**) ($CDCl_3$, 600 MHz)……..243

Figure 4.99 ^{13}C JMOD spectrum of compound (**117**) ($CDCl_3$, 150 MHz)…..244

Figure 4.100 (**A**) HSQC spectrum, (**B**) Enlarged HSQC spectrum – Part I, and (**C**) Enlarged HSQC spectrum – Part II of compound (**117**)……246

Figure 4.101 (**A**) COSY spectrum; (**B**) Enlarged COSY spectrum – Part I, and (**C**) Enlarged COSY spectrum – Part II of compound (**117**)……..248

Figure 4.102 (**A**) HMBC spectrum; (**B**) Enlarged HMBC spectrum – Part I, (**C**) Enlarged HSQC spectrum – Part II, (**D**) Enlarged HMBC spectrum – Part III and (**E**) Enlarged HMBC spectrum – Part IV of compound (**117**)…….251

Figure 4.103 Selected COSY and HMBC correlations of compound (**117**)…..252

Figure 4.104 (**A**) NOESY spectrum and (**B**) Enlarged NOESY spectrum – Part I of compound (**117**)……..254

Figure 4.105 Selected NOESY correlations of compound (**117**)……..254

Figure 4.106 ECD spectrum of compound (**117**) (MeOH, 20 µg/mL)……..255

Figure 4.107 Projection of mitragynine oxindole B (**117**), with the displacement ellipsoids drawn at the 50% probability level……...255

Figure 4.108 Proposed structure of compound (**117**)…….256

Figure 4.109 HR-ESI-MS (positive mode) spectrum of compound (**88**).....256

Figure 4.110 (**A**) GC-MS chromatogram and (**B**) EI-MS spectrum of compound (**88**)……...258

Figure 4.111 UV spectrum of compound (**88**) in methanol.....259

Figure 4.112 IR spectrum of compound (**88**) (KBr)……..260

Figure 4.113 ^{1}H NMR spectrum of compound (**88**) ($CDCl_3$, 500 MHz)……...265

Figure 4.114 ^{13}C NMR spectrum of compound (**88**) ($CDCl_3$, 125 MHz)……..266

Figure 4.115 (**A**) HSQC spectrum, (**B**) Enlarged HSQC spectrum – Part I, (**C**) Enlarged HSQC spectrum – Part II and (**D**) Enlarged HSQC spectrum – Part III of compound (**88**)……..268

Figure 4.116 (**A**) HMBC spectrum, (**B**) Enlarged HMBC spectrum – Part I, (**C**) Enlarged HMBC spectrum – Part II and (**D**) Enlarged HMBC spectrum – Part III of compound (**88**)……...271

Figure 4.117 Selected COSY and HMBC correlations of compound (**88**)……272

Figure 4.118 (**A**) COSY spectrum, (**B**) Enlarged COSY spectrum – Part I and (**C**) Enlarged HSQC spectrum – Part II of compound (**88**)…….……273

Figure 4.119 ECD spectrum of compound (**88**) (MeOH, 20 µg/mL)…….274

Figure 4.120 Proposed structure of compound (**88**)……...274

Figure 4.121 (**A**) GC-MS chromatogram of fraction F6, (**B**) EI-MS spectrum of peak 6a, (**C**) EI-MS spectrum of peak 6b, (**D**) EI-MS spectrum of peak 6c, and (**E**) EI-MS spectrum of peak 6d……277

Figure 4.122 HR-ESI-MS (positive mode) spectrum of compound (**90**)……...278

Figure 4.123 (**A**) GC-MS chromatogram and (**B**) EI-MS spectrum of compound (**90**)……...279

Figure 4.124 UV spectrum of compound (**90**) in methanol……280

Figure 4.125 ^{13}C NMR spectrum of compound (**90**) ($CDCl_3$, 150 MHz)……..284

Figure 4.126 (**A**) HSQC spectrum, (**B**) Enlarged HSQC spectrum – Part I, and (**C**) Enlarged HSQC spectrum – Part II of compound (**90**)…….286

Figure 4.127 ^{1}H NMR spectrum of compound (**90**) ($CDCl_3$, 600 MHz)……287

Figure 4.128 (**A**) COSY spectrum, (**B**) Enlarged COSY spectrum – Part I, and (**C**) Enlarged COSY spectrum – Part II of compound (**90**)…….289

Figure 4.129 (**A**) HMBC spectrum, (**B**) Enlarged HMBC spectrum – Part I, (**C**) Enlarged HMBC spectrum – Part II, and (**D**) Enlarged HMBC spectrum – Part III of compound (**90**)……..292

Figure 4.130 Selected COSY and HMBC correlations of compound (**90**)……293

Figure 4.131 Proposed structure of compound (**90**)……..293

Figure 4.132 Positive ion HR-ESI-MS of compound (**146**)……294

Figure 4.133 (**A**) GC-MS chromatogram and (**B**) EI-MS spectrum of compound (**146**)…….295

Figure 4.134 UV spectrum of compound (**146**) in methanol…….295

Figure 4.135 ^{1}H NMR spectrum of compound (**146**) ($CDCl_3$; 600 MHz)…….300

Figure 4.136 ^{13}C NMR spectrum of compound (**146**) ($CDCl_3$; 150 MHz)…….301

Figure 4.137 (**A**) HSQC spectrum, (**B**) Enlarged HSQC spectrum – Part I, and (**C**) Enlarged HSQC spectrum – Part II of compound (**146**)……..303

Figure 4.138 (**A**) HMBC spectrum, (**B**) Enlarged HMBC spectrum – Part I, (**C**) Enlarged HMBC spectrum – Part II and (**D**) Enlarged HMBC spectrum – Part III of compound (**146**)……306

Figure 4.139 (**A**) COSY spectrum, (**B**) Enlarged COSY spectrum – Part I, and (**C**) Enlarged COSY spectrum – Part II of compound (**146**)……...308

Figure 4.140 Selected COSY and HMBC correlations of compound (**146**)…..306

Figure 4.141 (**A**) NOESY spectrum and (**B**) Enlarged NOESY spectrum – Part I of compound (**146**)……...310

Figure 4.142 Selected NOESY correlations of compound (**146**)……..…..311

Figure 4.143 Proposed structure of compound (**146**)…….311

Figure 4.144 Comparison of chemical structures of newly discovered 17(*Z*)-speciociliatine (**146**) and the synthetized 17(*Z*)-mitragynine (**147**) (Kruegel et al., 2016)……312

Figure 4.145 HRESI-MS (positive mode) spectrum of compound (**98**)……313

Figure 4.146 ^{1}H NMR spectrum of compound (**98**) (CD_3OD, 600 MHz)…….318

Figure 4.147 ^{13}C NMR spectrum of compound (**98**) (CD_3OD, 150 MHz)…….319

Figure 4.148 (**A**) DEPT 135 and (**B**) DEPT 90 spectra of compound (**98**)……320

Figure 4.149 (**A**) HSQC spectrum, (**B**) Enlarged HSQC spectrum – Part I, (**C**) Enlarged HSQC spectrum – Part II, and (**D**) Enlarged HSQC spectrum – Part III of compound (**98**)……...323

Figure 4.150 (**A**) HMBC spectrum, (**B**) Enlarged HMBC spectrum – Part I, (**C**) Enlarged HMBC spectrum – Part II, (**D**) Enlarged HMBC spectrum – Part III, and (**E**) Enlarged HSQC spectrum – Part IV of compound (**98**)……...……327

Figure 4.151 (**A**) COSY spectrum, (**B**) Enlarged HSQC spectrum – Part I and (**C**) Enlarged HSQC spectrum – Part II, of compound (**98**)……329

Figure 4.152 Selected COSY and HMBC correlations of compound (**98**)…….330

Figure 4.153 1D NOESY spectrum of compound (**98**) (CD_3OD, 600 MHz)….331

Figure 4.154 Selected 1D NOE correlations of compound (**98**)…….332

Figure 4.155 Proposed structure of compound (**98**)……...……332

Figure 4.156 (**A**) HRESI-MS (positive mode) and (**B**) HR-ESI-MS/MS (positive mode) spectra of compound (**116**)……335

Figure 4.157 Proposed HRESI-MS/MS fragmentation mechanism of compound (**116**)…….336

Figure 4.158 UV spectrum of compound (**116**) in methanol…….334

Figure 4.159 ^{1}H NMR spectrum of compound (**116**) ($CDCl_3$, 600 MHz)…….341

Figure 4.160 ^{13}C NMR JMOD spectrum of compound (**116**) ($CDCl_3$, 150 MHz)……342

Figure 4.161 (**A**) HSQC spectrum, (**B**) Enlarged HSQC spectrum – Part I, (**C**) Enlarged HSQC spectrum – Part II, and (**D**) Enlarged HSQC spectrum – Part III of compound (**116**)…….344

Figure 4.162 (**A**) COSY spectrum, (**B**) Enlarged COSY spectrum – Part I and (**C**) Enlarged COSY spectrum – Part II of compound (**116**)……346

Figure 4.163 (**A**) HMBC spectrum, (**B**) Enlarged HMBC spectrum – Part I, (**C**) Enlarged HMBC spectrum – Part II, and (**D**) Enlarged HMBC spectrum – Part III, and of compound (**116**)…….349

Figure 4.164 Selected COSY and HMBC correlation of compound (**116**)……349

Figure 4.165 (A) NOESY spectrum and (B) Enlarged NOESY spectrum – Part I of compound (**116**)……...351

Figure 4.166 Selected NOESY correlations of compound (**116**)……..…351

Figure 4.167 ECD spectrum of compound (116) (MeOH, 20 µg/mL)……..352

Figure 4.168 Comparisons of ECD spectra of compound (**116**) (7*S*), mitrafoline (**125**) (7*S*), and mitragynine oxindole B (**117**) (7*R*) (MeOH, 20 µg/mL)…….352

Figure 4.169 Proposed structure for compound (**116**)……...353

Figure 4.170 Chemical structure of the isolated alkaloids from fractions F2-F6.....354

Figure 4.171 TLC profiles of major alkaloids isolated from fractions F2-F6 developed using (**A**) solvent system I and (**B**) solvent system II [Denotation – MG (**87**), SG (**89**), SC (**88**), PAY (**91**), CR (**81**), CA (**101**), CB (**82**), MB (**117**), 7-OH (**94**)]…….356

Figure 4.172 GC-MS chromatograms of (**A**) paynantheine (**91**), (**B**) corynantheidine (**101**), (**C**) mitragynine (**87**), (**D**) mitraciliatine (**90**), (**E**) speciociliatine (**88**) and (**F**) speciogynine (**89**)……..358

Figure 4.173 EI-MS spectra of (**A**) speciociliatine (**88**), (**B**) mitragynine (**87**), (**C**) speciogynine (**89**), (**D**) mitraciliatine (**90**), (**E**) paynantheine (**91**) and (**F**) corynantheidine (**101**)…….360

Figure 4.174 GC-MS chromatograms of (**A**) corynoxine (**81**), (**B**) corynoxine B (**82**) and (**C**) mitragynine oxindole B (**117**)……..361

Figure 4.175 EI-MS spectra of (**A**) corynoxine (**81**), (**B**) corynoxine B (**82**), and (**C**) mitragynine oxindole B (**117**)……362

Figure 4.176 GC-MS chromatograms of (A) an alkaloid extract of M. speciosa and (B) the enlarged region from 16.00 to 26.00 min……...363

Figure 4.177 Percentage of inhibition of the alkaloid extract and major alkaloids from *M. speciosa* at 100 µg/mL……369

Figure 4.178 Comparison of chemical structures between *M. speciosa* alkaloids and harmala alkaloids……...373

Figure 4.179 Stereo structures of paynantheine (**91**) (3*S*) and (**92**) (3*R*)……375

Figure 4.180 Three-dimensional structure comparison of compounds (**81**), (**82**), (**101**) and huperzine A (AChE inhibitor) (most stable conformation, ChemDraw 3D)...…….376

Figure 4.181 Three-dimensional structure comparison of compounds (**87**), (**88**), (**89**), (**90**), and (**91**) (most stable conformation, Chemdraw 3D)..378

Figure 4.182 The structure-inhibition relationships of *M. speciosa* alkaloids towards AChE, with mitragynine (**87**) and (**117**) as examples…380

Figure 4.183 The structure-inhibition relationships of *M. speciosa* alkaloids towards BChE, with mitragynine (**87**) and (**117**) as examples….381

Figure 4.184 Lineweaver-Burk plots of (**A**) corynoxine (**81**) on AChE, and (**B**) speciogynine (**89**) on BChE……..383

Figure 4.185 Binding orientations and interactions of (**A**) corynoxine (**81**) with protein residues at the active site of AChE, (**B**) paynantheine (**91**) with protein residues at the active site of AChE, and (**C**) speciogynine (**89**) with protein residues at the active site of BChE……387

Figure 4.186 Three-dimensional chemical structures for morphine and corynoxine (**81**)……391

LIST OF SYMBOLS AND ABBREVIATIONS

α	Alpha
Aβ	Amyloid beta
β	Beta
δ	Chemical shift
ó	Delta
κ	Kappa
π	Pi
λ_{max}	Lambda max (absorption max)
μ	Mu
J	Coupling constant
$\approx$	Approximately
1D	One-dimensional
2D	Two-dimensional
3D	Three-dimensional
5-HT	Serotonin
AD	Alzheimer's Disease
AR	Analytical grade
AChE	Acetylcholinesterase
ATCI	Acetylthiocholine iodide
BChE	Butyrylcholinesterase
bd	Broad doublet
bs	Broad singlet
BTCI	Butyrylthiocholine iodide
^{13}C	Carbon

$CHCl_3$	Chloroform
CH_3COOH	Acetic acid
$CDCl_3$	Deuterated chloroform
CD_3OD	Deuterated methanol
CNS	Central Nervous System
COSY	Homonuclear Shift Correlation Spectroscopy
DCM	Dichloromethane
d	Doublet
dd	Doublet of doublet
dt	Doublet of triplet
DEPT	Distortionless Enhancement by Population Transfer
(*E*)	*Trans* configuration
EC_{50}	Half maximal effective concentration
ECD	Electronic Circular Dichroism
E_{max}	Maxima Efficacy
ED_{50}	the dose of a medication that produces a specific effect in 50% of the population that has been administered that dose
EI	Electron ionization
ESI	Electron-sprayed ionization
EtOAc	Ethyl acetate
FT	Fourier Transform
GC-MS	Gas chromatography-mass spectrometer
GPCR	G-protein coupled receptor
^1H	Proton
[^3H]	tritiated
HMBC	Heteronuclear Multiple Bond Coherence
hMOR	Human mu opioid receptor

hKOR	Human kappa opioid receptor
hDOR	Human delta opioid receptor
HR	High Resolution
HSQC	Heteronuclear Single Quantum Correlation
Hz	Hertz
i.e.	that is
IR	Infrared Spectroscopy
Km	Michaelis constant
Ki	inhibition constant
IC_{50}	50% of inhibition concentration
JMOD	J-modulation
LC-MS	Liquid chromatography-mass spectrometer
m	multiplet
MeOH	methanol
mM	millimolar
M. diversifolia	*Mitragyna diversifolia*
M. speciosa	*Mitragyna speciosa*
M. rotundifolia	*Mitragyna rotundifolis*
MS	Mass spectrometry
MS/MS	Tandem mass spectrometry
NH_3OH	Ammonium hydroxide
nM	Nano molar
NMR	Nuclear Magnetic Resonance
NOE	Nuclear Overhauser Effect
NOESY	Nuclear Overhauser Effect Spectroscopy
Q-TOF	Quadrupole- Time of Flight
R_f	Retention factor

s	singlet
SD	Standard deviation
SEM	Standard error mean
t	triplet
TCM	Traditional Chinese Medicine
TLC	Thin-layer chromatography
U. hirsuta	*Uncaria hirsuta*
U. macrophylla	*Uncaria macrophylla*
U. rhynchophylIa	*Uncaria rhynchophylIa*
U. sessilifructus	*Uncaria sessilifructus*.
U. sinensis	*Uncaria sinensis*
UN	United Nations
US	United States
UV	Ultra-violet
µg/mL	Microgram per mililiter
µM	Micro molar
v/v	Volume by volume
V_{max}	Maximum velocity
(*Z*)	*Cis* configuration

KAJIAN MENGENAI KIMIA, AKTIVITI ANTIKOLINESTERASE DAN KETOKSIKAN ALKALOID *Mitragyna speciosa* (KRATOM)

ABSTRAK

Mitragyna speciosa (Korth) Havil. merupakan tumbuhan asli Malaysia yang digunakan secara tradisi untuk merawat kesakitan, kencing manis, hipertensi dan ketagihan dadah. Ia juga digunakan sebagai minuman tonik untuk meningkatkan kewaspadaan, perhatian dan prestasi kerja dalam kalangan buruh dan petani. Kebanyakan aktiviti farmakologi yang direkodkan untuk *M. speciosa* berfokus pada aktiviti berkaitan opioid. Kajian mengenai potensi kesan terapeutik *M. speciosa* ke atas sistem neurotransmisi kolinergik masih kurang. Terdapat hanya satu kajian yang melaporkan aktiviti antikolinesterase untuk ekstrak metanol dan mitraginin yang disediakan daripada *M. speciosa* Thailand. Oleh itu, kajian ini bertujuan untuk mengenal pasti sebatian daripada *M. speciosa* yang berpotensi untuk merencat kolinesterase melalui pendekatan pemencilan berpandukan bioasai. Sejumlah tiga belas alkaloid, termasuk dua alkaloid yang baru, telah berjaya dipencilkan dan dicirikan daripada ekstrak alkaloid dengan menggunakan teknik kromatografik dan kaedah spektroskopi moden. Kesemua alkaloid yang telah dipencilkan adalah mitraginin (**87**), spesiosiliatin (**88**), spesioginin (**89**), mitrasiliatin (**90**), paynanthein (**91**), korinantheidin (**101**), korinosin (**81**), korinosin B (**82**), mitrafolin (**125**), mitraginin oksindol B (**117**), mitraginin oksindol A (**116**), 17(*Z*)-spesiosiliatin (**146**), dan spesiosiliatin *N*-oksida (**98**). Dua daripada kesemua alkaloid tersebut, 17(*Z*)-spesiosiliatin (**146**), dan spesiosiliatin *N*-oksida (**98**) merupakan sebatian baru daripada *M. speciosa*. Terutamanya, 17(*Z*)-spesiosiliatin (**146**) adalah isomer keempat mitragynine, selain (**88**), (**89**), dan (**90**). Struktur kimia untuk tiga oksindol luar biasa

(**125**), (**117**), dan (**116**), yang mempunyai sama ada kumpulan hidroksil atau metoksi digantikan pada kedudukan 9, juga dikaji semula, dan data NMR mereka dilaporkan buat kali pertama. Aktiviti antikolinesterase untuk kesemua alkaloid tersebut, termasuk aktiviti perencatan mereka pada kedua-dua isoform asetilkolinesteras (AChE) dan butirilkholinesterase (BChE), telah ditentukan. Kebanyakan alkaloid ini mempunyai aktiviti perencatan berkecenderungan kepada BChE, dan dianggap sebagai perencat BChE selektif. Antaranya, spesioginin (**89**) adalah perencat BChE yang paling berkesan, dengan nilai IC_{50} sebanyak 5.48 μM. Ia kemudian dikenalpasti sebagai perencat mod campuran daripada kajian kinetik. Sebaliknya, korinosin (**81**) merupakan perencat AChE yang paling berkesan dan selektif (IC_{50} = 6.12 μM) di antara semua alkaloid yang telah diuji. Berdasarkan kajian kinetik, korinosin (**81**) dikenalpasti sebagai perencat mod campuran. Perencat kolinesterase (**81**), (**91**) dan (**89**) didapati mempunyai kesan toksik yang ringan ataupun yang boleh diabaikan ke atas semua jenis sel yang diuji ($IC_{50} \geq 50$ μM). Alkaloid-alkaloid ini juga mempunyai kebolehan pengikatan yang rendah pada reseptor μ-opioid, kecuali (**81**). Korinosin (**81**) mempunyai kebolehan pengikatan yang tinggi dan selektif pada reseptor μ-opioid, dengan nilai *Ki* sebanyak 16.4 nM. Ini menunjukkan bahawa (**81**) adalah calon yang berpotensi dalam pembangunan ubat opioid, di samping potensinya yang luar biasa sebagai perencat mod campuran untuk AChE.

STUDIES ON THE CHEMISTRY, ANTICHOLINESTERASE ACTIVITY AND TOXICITY OF *Mitragyna speciosa* (KRATOM) ALKALOIDS

ABSTRACT

Mitragyna speciosa (Korth) Havil. is a medicinal plant native to Malaysia, traditionally used to treat pain, diabetes, hypertension, and drug addiction. It is also consumed as a tonic beverage to enhance alertness, attention and working performance among labourers and farmers. Most pharmacological activities documented for *M. speciosa* focus on opioid-related activities. Research on the potential therapeutic effects of *M. speciosa* on the cholinergic neurotransmission system is still scarce. Only one study has reported the anticholinesterase activity of the methanol extract and mitragynine prepared from Thai *M. speciosa*. Therefore, this study aims to identify potential cholinesterase inhibitors from *M. speciosa* using a bioassay-guided isolation approach. A total of thirteen alkaloids were isolated and characterized from the alkaloid extract using modern chromatographic techniques and spectroscopic methods. The isolated alkaloids were mitragynine (**87**), speciociliatine (**88**), speciogynine (**89**), mitraciliatine (**90**), paynantheine (**91**), corynantheidine (**101**), corynoxine (**81**), corynoxine B (**82**), mitrafoline (**125**), mitragynine oxindole B (**117**), mitragynine oxindole A (**116**), 17(*Z*)-speciociliatine (**146**), and speciociliatine *N*-oxide (**98**). Two of these alkaloids, 17(*Z*)-speciociliatine (**146**) and speciociliatine *N*-oxide (**98**), are the new compounds from *M. speciosa*. Notably, 17(*Z*)-speciociliatine (**146**) is the fourth isomer of mitragynine (**87**), in addition to (**88**), (**89**) and (**90**). The chemical structures of three uncommon oxindoles (**125**), (**117**), and (**116**), which had either a hydroxyl or methoxy group replaced at position 9, were also revisited, and their NMR data were reported for the first time. The anticholinesterase activity of the isolated alkaloids,

which included their inhibitory activity on both acetylcholinesterase (AChE) and butyrylcholinesterase (BChE) isoforms, was evaluated. Most of the isolated alkaloids showed predominant inhibitory activity on BChE, which are regarded as selective BChE inhibitors. Speciogynine (**89**) was the most potent BChE inhibitor, with an IC_{50} value of 5.48 µM. It was later identified as a mixed-mode inhibitor from the kinetic study. On the other hand, corynoxine (**81**) was the most potent and selective AChE inhibitor (IC_{50} = 6.12 µM). Based on the kinetic study, (**81**) was identified as a mixed-mode inhibitor. Cholinesterase inhibitors (**81**), (**91**) and (**89**) were found to have mild or negligible toxic effects on all the tested cell lines ($IC_{50} \geq 50$ µM). These alkaloids also had a low binding affinity to human µ-opioid receptors, except (**81**). Corynoxine (**81**) had a high and selective binding affinity to human µ-opioid receptors, with a *Ki* value of 16.4 nM. This suggests that (**81**) is a potential candidate for opioid drug development, in addition to its exceptional potential as a mixed-mode AChE inhibitor.

CHAPTER ONE

INTRODUCTION

1.1 Overview

Alzheimer's disease (AD) is the most common form of dementia associated with ageing in older individuals. It is defined as a gradual deterioration in cognitive abilities and memory function (Zeng et al., 2021a; 2021b). Based on United Nations (UN) estimates, the population of individuals with AD is projected to increase dramatically from 25.5 million in 2000 to an expected 114 million by 2050 (Wimo et al., 2003). AD is characterized by extracellular amyloid-β plaques, intracellular tau buildup, and gradual death of cholinergic neurons (Scheltens et al., 2016; Asaad & Lee, 2018). Sadly, many clinical trials that focused on a specific protein maker, such as amyloid-β and tau, were unsuccessful (Mehta et al., 2017).

At present, the only anti-AD drugs that have received clinical approval are cholinesterase inhibitors (e.g., rivastigmine, donepezil, and galantamine) or *N*-methyl-d-aspartate (NMDA) receptor antagonist (memantine) (Lai et al., 2022). These drugs are used to improve cognitive function and reduce behavioural disabilities among mild or moderate AD patients. Cholinesterase inhibitors inhibit the activity of cholinesterase by preventing it from breaking down acetylcholine into acetate and choline by hydrolysis. This helps increase the level of acetylcholine and, subsequently, its duration of action in the brains of AD patients. Consequently, this supports their daily functions, including alertness, focus, memory, learning and motor movement (Shoja et al., 2016; Kong et al., 2021). However, cholinesterase inhibitors are regarded as symptomatic medications as they cannot stop or reverse the disease's progression

(Kong et al., 2021). In addition, many first-generation cholinesterase inhibitors, including tacrine (Cognex), have been discontinued due to liver toxicity (Park et al., 2015). Due to the scarcity of clinically used cholinesterase inhibitors, there is a continuing effort to discover more potent and safer alternatives, particularly from medicinal plants.

Traditional healers have long employed medicinal plants to treat various forms of dementia, including AD. Several Ayurvedic and Traditional Chinese Medicine (TCM) herbs, including *Gingko biloba*, *Panax ginseng*, *Huperzia serrata*, *Centella asiatica*, and *Bacopa monnieri*, have been used for centuries to enhance intelligence, cognition, and memory (Tewari et al., 2018; Farooqui, 2019). However, the therapeutic use and clinical studies of these medicinal plants are only limited to crude drugs or standardized extracts, except for huperzine A from *Huperzia serrata* (Li et al., 2021). Huperzine A (a lycopodium alkaloid) is a potent cholinesterase inhibitor isolated from the Chinese club moss, *Huperzia serrata*, which is licensed in China as a medication for AD (Li et al., 2021). Huperzine A is available in the United States (US) as an herbal supplement. Nevertheless, the Food and Drug Administration (FDA) has not approved it for treating AD (Thu et al., 2019).

In TCM, *Uncaria rhynchophylla*, also known as Gou-Teng and Chinese Cat's Claw, has garnered study interest in its potential to treat age-associated cognitive disorders, including AD (Lan et al., 2018; Zeng et al., 2021a). The major bioactive compounds of *U. rhynchophylla* are corynanthe-type alkaloids, including hirsutine, hirsuteine, geissoschizine methyl ether, rhynchophylline, isorhynchophylline etc. (Xian et al., 2012; Wu et al., 2020). These alkaloids exert neuroprotective effects through multiple mechanisms, such as NMDA antagonistic activity, inhibition of Aβ aggregation, anti-neuroinflammation, cholinesterase inhibitory activity, etc. (Wu et al.,

2020; Zeng et al., 2021a). However, the clinical trials examining the cognitive-enhancing activities of *U. rhynchophylla* and its primary active alkaloid, rhynchophylline, are ongoing and have not been concluded (Yang et al., 2020).

Mitragyna is a group of perennial trees belonging to the Rubiaceae family, comprising seven members across Asia and Africa. Taxonomically, *Mitragyna* is closely related to the genera *Uncaria* and *Nauclea*, which are all under the Naucleeae tribe. Three species of this genus are recognized in Malaysia, including *Mitragyna speciosa*, *Mitragyna diversifolia* and *Mitragyna rotundifolia* (Brown et al., 2017; Ahmad et al., 2022). Among these, *M. speciosa* is the plant of interest due to its stimulant- and opioid-like activities. *M. speciosa*, locally known as Ketum, Biak-Biak (Malaysia) or Krathum (Thailand), is traditionally used in Malaysia and Thailand to treat pain, opioid addiction, hypertension, and diabetes. It is also consumed as a general tonic to improve sexual performance, mood, alertness/focus, sociability, and cognitive performance among manual labourers (Warner et al., 2016; Singh et al., 2017; Ramanathan & McCurdy, 2020). In the US, *M. speciosa* is more commonly referred to as 'Kratom', which has been marketed as herbal supplements in various forms (i.e., shredded/powdered leaves, encapsulated powder/extract) and 'strains' (i.e., Red Bali, Maeng Da, Green Malay, White Borneo) (Raffa, 2015; Brown et al., 2017; Boffa et al., 2018). Early studies of the phytochemicals of *M. speciosa* reported it to contain more than 40 corynanthe-type indole and oxindole alkaloids, which are all structurally related to *Uncaria* alkaloids (Brown et al., 2017; Flores-Bocanegra et al., 2020). Mitragynine, an indole alkaloid of the corynanthe class, is the main constituent in *M. speciosa* leaves, constituting about 66% of the alkaloid content. Other significant alkaloids are speciogynine, speciociliatine and paynanthiene, which comprise approximately 20% of total alkaloid extract (Gogineni et al., 2014; Kruegel et al.,

2019). In contrast to indoles, oxindoles are minor alkaloids, and their presence in the plant material is often inconsistent and disregarded (Shellard et al., 1978b; 1978c; Boffa et al., 2018). Studies of the pharmacological activities of *M. speciosa* have primarily focused on opioid-like activities, such as antinociceptive activity, as well as the associated adverse effects, including toxicity, drug metabolism, withdrawal symptoms, abuse potentials and cognitive impairment of mitragynine and its oxidative derivative – 7-hydroxy mitragynine (Kruegel et al., 2016; Yusoff et al., 2016; Kong et al., 2017; Hassan et al., 2019; Kruegel et al., 2019; Chakraborty et al., 2021; Hill et al., 2022). In recent years, research on *M. speciosa* has expanded to explore the other psychopharmacological activities (i.e., mood-enhancing, antidepressant, and antianxiety activities) of mitragynine or, in some cases, include its indole congeners, such as paynantheine, speciogynine, and speciociliatine, to understand better the plant's overall therapeutic effect (Buckhalter et al., 2021; León et al., 2021). However, the contributing role of other *M. speciosa* alkaloids, specifically the oxindoles, in the overall pharmacological action of *M. speciosa* is yet unknown.

1.2 Problem Statement

According to the literature, studies on the phytochemistry of *M. speciosa* have primarily focused on corynanthe-type indoles, such as mitragynine and its diastereomers. Rhynchophylline- and 9-hydroxyrhynchophylline-type alkaloids are among the common corynanthe-type oxindoles that have been isolated from the plant, and some of them can also be found in *Uncaria* plants (Ali et al., 2014; Brown et al., 2017). Surprisingly, the occurrence of 9-methoxyrhynchophylline-type alkaloids in *M. speciosa* has rarely been reported, and many of their chemical structures have not been thoroughly characterized (Trager et al., 1968; Beckett et al., 1969; Shellard et al.,

1978a; 1978b; 1978c). These oxindoles are taxonomically important to *M. speciosa* as they are the oxidation products of mitragynine-type alkaloids following the biosynthesis pathway of *Mitragyna* alkaloids. Unfortunately, the psychopharmacological activities of oxindole alkaloids, particularly at central opioid receptors, are still poorly understood.

In Malaysia, *M. speciosa* is widely consumed as a tonic to improve cognitive performance, such as alertness and focus, in addition to its primary function of treating pain and opioid addiction. Most pharmacological activities documented for *M. speciosa* focus on opioid-related activities. Research on the potential therapeutic effects of *M. speciosa* on the cholinergic neurotransmission system is still scarce. During our ongoing exploration of new cholinesterase inhibitors from medicinal plants in Malaysia, we found that the methanol and alkaloid extracts obtained from the leaves of *M. speciosa* had strong inhibitory effects on the acetylcholinesterase (AChE) enzyme. The IC_{50} values for these extracts were 35.52 and 6.12 µg/mL, respectively. The AChE inhibitory activity of *M. speciosa* and mitragynine has only been described once, of which the plant material was collected from Thailand. The Thai-origin leaf extract and mitragynine were reported as weak AChE inhibitors (IC_{50} values > 100 µg/mL) (Innok et al., 2021). Therefore, it is hypothesized that other alkaloids, but not mitragynine, are responsible for the potent AChE inhibitory activity of Malaysian *M. speciosa* extracts, which may not be found in Thai *M. speciosa* extract. Additionally, no studies yet report the butyrylcholinesterase (BChE) inhibitory potential of *M. speciosa* alkaloids. Although *M. speciosa* extract seems to be a promising source of opioid ligands and cholinesterase inhibitors, the safety of its alkaloids is a subject of considerable concern, notably regarding toxicity and cognitive impairment, as seen with mitragynine (Saidin et al., 2015; Yusoff et al., 2016; Kong et al., 2017). All these

have piqued our interest in studying this plant further and finding its bioactive and non-toxic alkaloids for treating AD.

1.3 Research Objectives

The present study was designed for three main research goals. The first goal was to extract, isolate and characterize the bioactive alkaloids from the leaves of *M. speciosa* (objectives I and II). Subsequently, the second goal was to evaluate the cholinesterase inhibitory activity (AChE and BChE) of the major alkaloids, including their structure-activity relationships (SARs) and molecular docking study (objectives III to IV). Lastly, the major alkaloids were tested for their possible adverse effects, including their binding affinities at opioid receptors and toxic effects on selected cell lines derived from major organs involved in the absorption, distribution, metabolism, and excretion (ADME) of a drug (objectives V and VI).

I. To extract, fractionate and isolate the alkaloid constituents of *M. speciosa* using a combined analytical and bioassay-guided isolation approach,
II. To characterize the isolated alkaloids using various spectroscopic methods (FT-IR, ECD, UV, 1D and 2D NMR, GC-MS, and LC-MS),
III. To evaluate *in vitro* cholinesterase inhibitory activities of the major isolated alkaloids and their structure-activity relationships (SARs),
IV. To obtain structure insight into bioactive alkaloids as potential cholinesterase enzyme inhibitors using a molecular docking approach,
V. To evaluate the radioligand-binding affinity of major isolated alkaloids at opioid receptors,

VI. To evaluate the cytotoxicity of the major isolated alkaloids against a panel of cell lines representing the major organs.

1.4 Experiment design

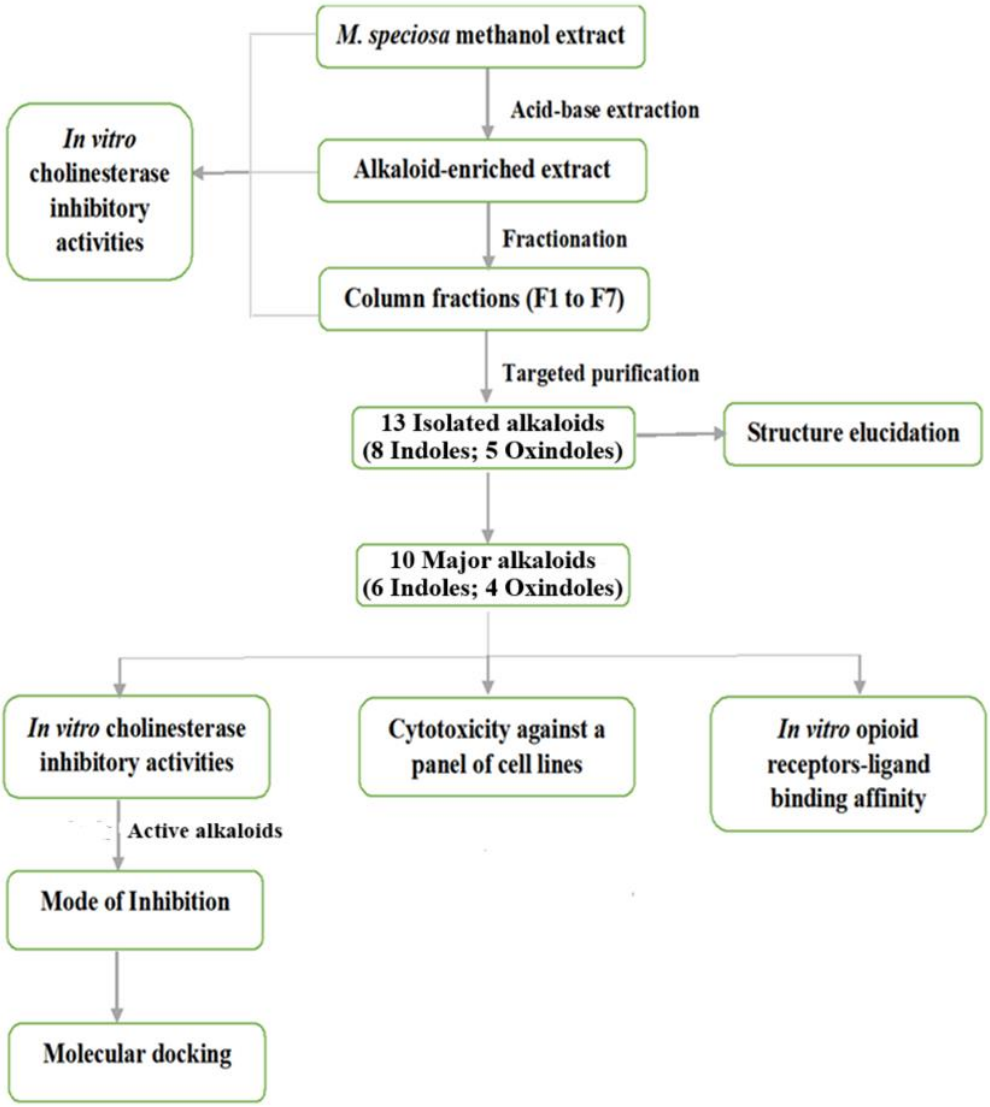

Figure 1.1 Flow chart of the designed study

CHAPTER TWO

LITERATURE REVIEW

2.1 Alzheimer's disease (AD)

Alzheimer's disease (AD) is the most common dementia among older adults, often associated with slow but progressive loss of synaptic neurons (Zeng et al., 2021a). According to United Nations (UN) estimates, the number of people with AD will exponentially rise from 25.5 million in 2000 to an anticipated 114 million in 2050 (Wimo et al., 2003). This disease affects the patient's cognitive and behavioural functions, which can be clustered into three categories: (I) mild AD, (II) moderate AD and (III) severe AD, depending on the disease's conditions and symptoms. Patients suffering from cognitive and executive dysfunction are in the first category – mild AD. Memory loss, communication disturbance, difficulty in planning and loss of coordination skills are the typical symptoms in this category. The second category is moderate AD, in which the patients have progressive memory loss and confusion. In some cases, the patients also experience psychiatric problems and behavioural changes, such as mood swings, depression, paranoia, and hallucinations, and may behave aggressively (Lopez et al., 2003). The third category is the total loss of a patient's ability to handle and perform daily activities, which is known as severe AD. However, AD starts far earlier before the signs can be detected. The early stage of AD, also known as preclinical AD, comprises a long asymptomatic period with histopathological hallmarks, but there is no evidence of cognitive or functional decline (Dubois et al., 2010). Asymptomatic AD can present for years, depending on the patients, typically 6-10 years, while the risk of progression can vary depending on age,

sex, and apolipoprotein status (Insel et al., 2019; Vermunt et al., 2019; Cho et al., 2021). Studies showed that not all people with preclinical AD would develop AD; only about 20-30 % of preclinical AD would develop into cognitive impairment (Vermunt et al., 2019; Cho et al., 2021).

2.2 Neuropathological hallmarks of AD

Alois Alzheimer was the first scientist to discover AD in 1907, and he detected an abnormality in the brain of a patient experiencing memory loss and personality abnormalities. In his report, many abnormal clumps and tangled bundles of fibres were found in the patient's brain, which are later known as amyloid plaques and neurofibrillary or tau tangles, respectively. These two misfolded proteins are now widely used as biomarkers to diagnose AD (Veitch et al., 2019).

The main neuropathological hallmarks or characteristics of AD are the existence of senile plaques, neurofibrillary tangles, and dystrophic neurites together with significant neuronal and synaptic loss in the brain of AD patients (Heneka et al., 2005). Two main proteins are involved in the pathogenesis of AD: β-amyloid (Aβ) and tau (Agarwal et al., 2021). During the early stage of AD, the brain undergoes slow but toxic changes, in which Aβ protein abnormally accumulates and forms senile plaques at the extracellular brain parenchyma. In some cases, the formation of neurofibrillary tangles is also observed within the neuron due to the abnormal phosphorylation of microtubule-associated tau protein in the brain cells of AD patients (Ahmed et al., 2010). The aggregations of Aβ and tau proteins trigger synaptic failure, mitochondria dysfunction, and activation of microglia and astrocytes, leading to chronic oxidative stress and inflammation (Heneka et al., 2015). These further induce the death of healthy neurons and cause the shrinkage of the hippocampus and entorhinal cortex,

which are the brain regions responsible for memory and cognition. The damage is prevalent at the late stage of AD, and the whole brain tissue has shrunk significantly compared to the healthy one (Figure 2.1) (DeTure & Dickson, 2019). The toxic events of AD further give rise to three main hypotheses: (i) the amyloid hypothesis, (ii) the tau hypothesis and (iii) the cholinergic hypothesis in the search for more effective anti-AD drugs.

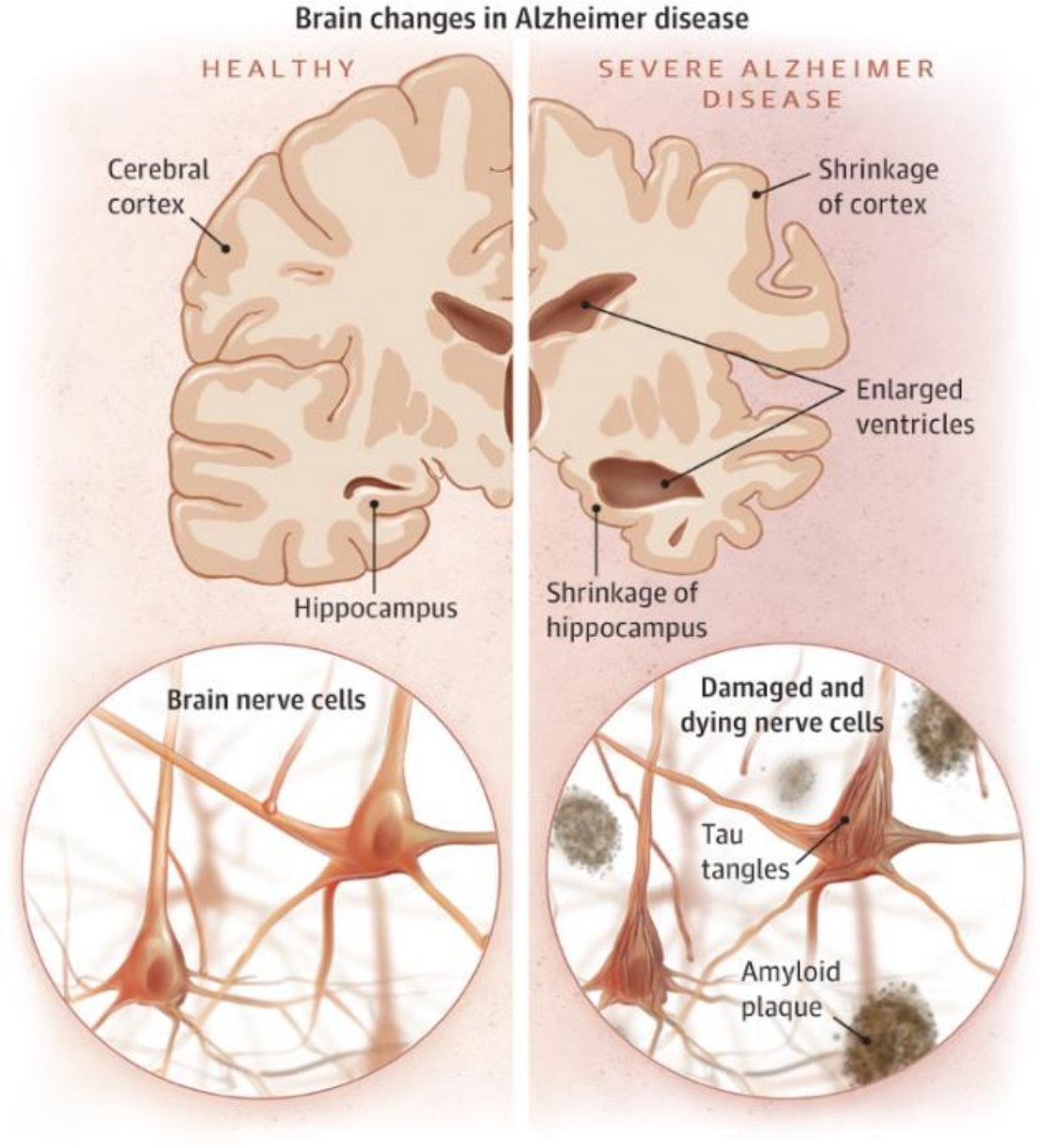

Figure 2.1 The brain region of a healthy person and AD patient (Adopted from DeTure & Dickson, (2019))

2.2.1 Amyloid hypothesis

The amyloid hypothesis was first proposed by Hardy and Higgins in 1992 when they presented the accumulation of Aβ peptides in an AD patient's brain parenchyma, which then became the protein target for AD research until now. According to the amyloid hypothesis, Aβ plaque is the causative agent of AD development. In the cascade event of AD, Aβ first accumulates and forms extracellular senile plaques and further progresses into AD associated with the formation of neurofibrillary tangles, neuronal loss, vascular damage, and dementia (Selkoe & Hardy, 2016).

Aβ peptides are a group of misfolding proteins formed from the proteolytic cleavage of amyloid precursor protein (APP), an integral membrane glycoprotein primarily found in the brain. There are two major cleavage pathways of APP: α-path (non-amyloidogenic) and β-path (amyloidogenic) (Chow et al., 2010). In most cases, the enzyme α-secretase cleaves APP via the α-path to form a soluble extracellular fragment of sAPP-α, then split into a shorter but non-toxic p3 protein (Nunan & Small, 2000). However, in some cases, APP is cleaved by another enzyme, β-secretase, into an intermediate fragment, sAPP-β, following the amyloidogenic β-pathway. sAPP-β is then cleaved by β-secretase into Aβ, which are short-length but toxic peptides containing 38-43 amino acids. Two major Aβ peptides are formed in the brain: $A\beta_{1–40}$ and $A\beta_{1–42}$, of which the latter is the more toxic peptide (Pauwels et al., 2011).

2.2.2 Tau hypothesis

Tau is a microtubule-associated protein found in the brain, which is involved in the outgrowth and transport of axons and stabilization of axonal microtubules. Phosphorylation is the primary process for the attachment of tau protein to the microtubules (Arnsten et al., 2021). However, hyperphosphorylated tau protein was

later identified as the primary component of neurofibrillary tangles found in the brains of AD patients, which is the second lesion characteristic of AD (Dujardin et al., 2020). This leads to the tau hypothesis, in which structural modification of tau, such as hyperphosphorylation and aggregation, interrupts tau's function and induces neuronal death. Hyperphosphorylated tau protein usually accumulates in neural perikaryal cytoplasm, axons, and dendrites, forming paired helical filaments. AD has three phases of hyperphosphorylated tau: pre-tangle, mature neurofibrillary tangles, and extracellular tangles. In the pre-tangle phase, the hyperphosphorylated protein accumulates in the somatodendritic region without forming any paired helical filament. In the second phase, the tau filament rapidly deposits and forms the neurofibrillary tangles by displacing the nucleus into the soma's periphery. In the extracellular tangles phase, a large amount of filamentous tau protein deposits and forms more neurofibrillary tangles, causing progressive neuronal death in the brain (Fichou et al., 2019). The formation of tau tangles usually starts in the entorhinal cortex and hippocampus and then spreads to other brain regions in a predictable spatial pattern as AD progresses (Dujardin et al., 2020). However, most AD cases are sporadic and not associated with tau protein, suggesting that tau is a cofactor and not the main contributor to AD pathogenesis (Wegmann et al., 2021).

2.2.3 Cholinergic hypothesis

One of the critical events in AD is the severe loss of cholinergic neurons in the cholinergic forebrain region, associated with decreased levels of the neurotransmitter acetylcholine (**1**) and its biosynthesis enzyme, choline acetyltransferase (Kong et al., 2021). Acetylcholine is synthesized by choline and acetyl CoA enzyme with choline

acetyltransferase. Acetylcholine is the endogenous agonist at muscarinic and nicotinic cholinergic receptors that control learning and memory (Klinkenberg et al., 2011).

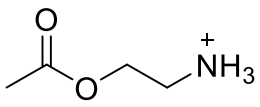

(**1**)

In addition, as AD progresses, brain cholinesterase (ChE) activity, the enzyme responsible for the breakdown of acetylcholine at neuromuscular junctions and cholinergic synapses, increases uncontrollably, further decreasing brain acetylcholine levels in AD patients. Therefore, it may be inferred that cholinergic neuronal loss and over-secretion of ChE are two main mechanisms reducing acetylcholine levels in the brains of AD patients, leading to memory loss and cognitive decline (Marucci et al., 2021). These phenomena support the cholinergic hypothesis that cholinergic augmentation may improve memory and cognition in AD patients by restoring brain acetylcholine levels with ChE enzyme inhibitors or agonists of muscarinic and nicotinic cholinergic receptors (Marucci et al., 2021). However, despite various preclinical candidates, no muscarinic or nicotinic agonist is available for treating AD.

2.3 Cholinesterase enzyme

Cholinesterase (ChE) is a serine hydrolase whose primary function is to catalyze the hydrolysis of the neurotransmitter acetylcholine into inactive products – choline (**2**) and acetic acid (**3**), thereby terminating neuronal transmission and synaptic signalling to prevent acetylcholine dispersion and activation of other adjacent receptors. This process is necessary for cholinergic neurons to return to their resting state after

activation (De Boer et al., 2021). The schematic mechanism of the acetylcholine hydrolysis reaction is shown in Figure 2.2.

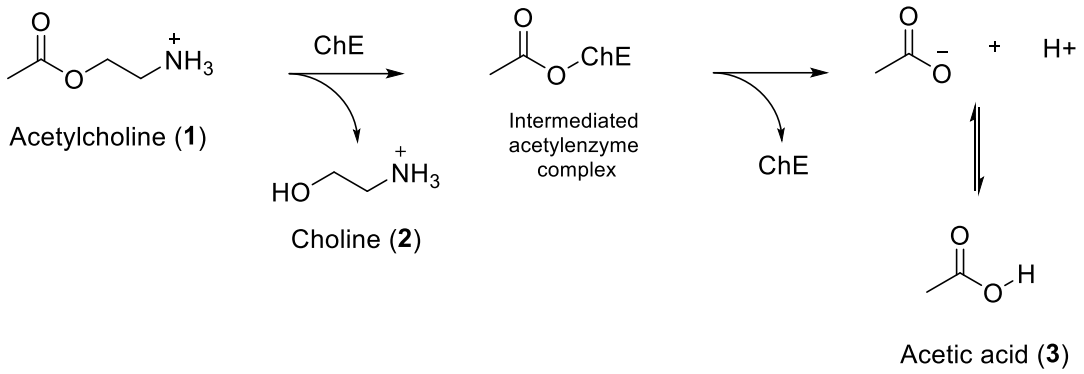

Figure 2.2 The reaction step of the hydrolysis of acetylcholine (**1**) by cholinesterase

Two types of ChE are found in the human brain: acetylcholinesterase (AChE) and butyrylcholinesterase (BChE) (Nordberg et al., 2013). AChE is primarily found in the brain and skeletal muscle, particularly at neural synapses and neuromuscular junctions. In contrast, BChE is produced by the liver and found in plasma. In the brain, BChE is predominantly localized to the glial cells. The specific substrate for AChE is acetylcholine, whereas BChE is a non-specific ChE that inhibits acetylcholine and other substrates, such as butyrylcholine (**4**) and propionylcholine (**5**) (Ha et al., 2020). The main difference between these two ChEs is their specificity for acetylcholine substrate: AChE cleaves acetylcholine faster than other choline esters. Conversely, BChE is less specific for acetylcholine but prefers to cleave butyrylcholine (**4**) faster. Butyrylcholine (**4**) is not naturally produced by the human body; it is a synthetic choline used as a specific substrate to differentiate AChE and BChE.

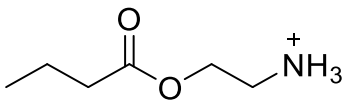

(**4**)

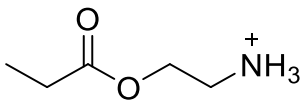

(**5**)

The protein structure of AChE and BChE are identical, and their amino acid sequence has a similarity of 65% despite being encoded by different genes (Soreq & Zakut, 1993). X-ray crystallography revealed that the molecules of AChE and BChE have an active hydrophobic gorge with two characteristic binding sites: catalytic and choline sites through which substrates enter (Stepankova & Komers, 2008). The presence of two large amino acids (Phe295 and Phe297) at the bottom of the AChE's gorge limits the available space for substrate binding in AChE, whereas, in BChE, these residues are replaced by two smaller amino acids-valine and leucine, creating additional space that allows the binding of larger substrates (Greig et al., 2001). According to Wiesner et al. (2007), there are five main domains of AChE's active site, which are the catalytic triad, the anionic subsite, the oxyanion hole, the acyl binding pocket and the peripheral anionic subsite (Wiesner et al., 2007; Div et al., 2010). BChE's active site only contains four main domains: the catalytic triad, the acyl pocket, the choline subsite, and the oxyanion hole (Lockridge et al., 2011).

In a healthy person, AChE contributes to approximately 90% of cholinesterase activity in the brain, and BChE the remaining 10% (Kong et al., 2021). However, as AD develops and progresses, the levels of BChE conversely increase by up to 90%, which is associated with a drastic decrease in AChE activity (Lai et al., 2022). Hence, BChE enzyme inhibition may also help restore brain acetylcholine levels, especially for severe AD. Given that AChE and BChE are involved in hydrolyzing acetylcholine, these enzymes have been used as the pharmacological targets for developing anti-AD drugs – cholinesterase inhibitors as recommended by the cholinergic hypothesis (Figure 2.4) (Lai et al., 2022).

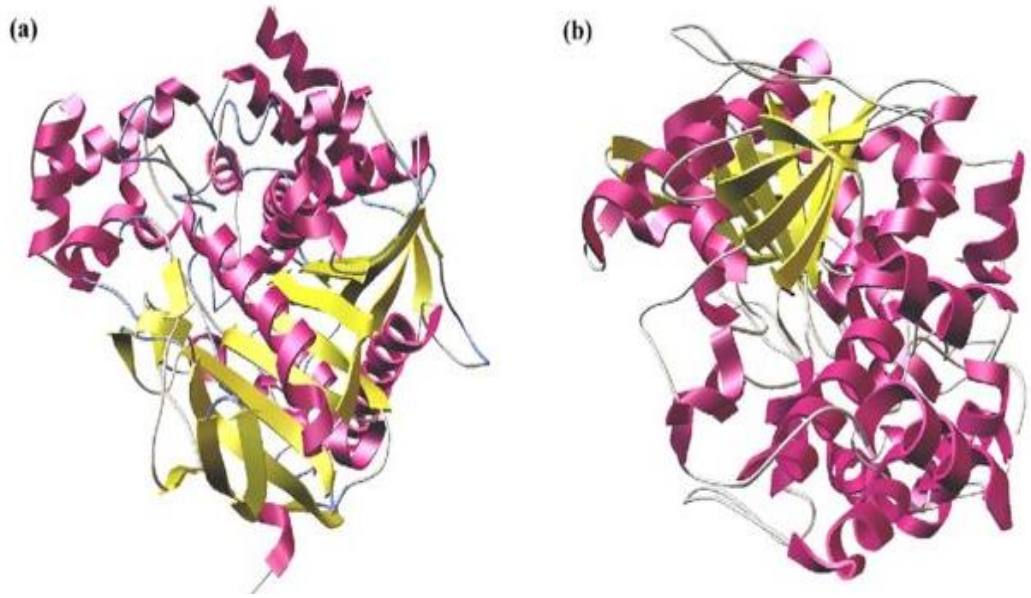

Figure 2.3 Protein structure of (**a**) acetylcholinesterase (AChE); (**b**) butyrylcholinesterase (BChE)

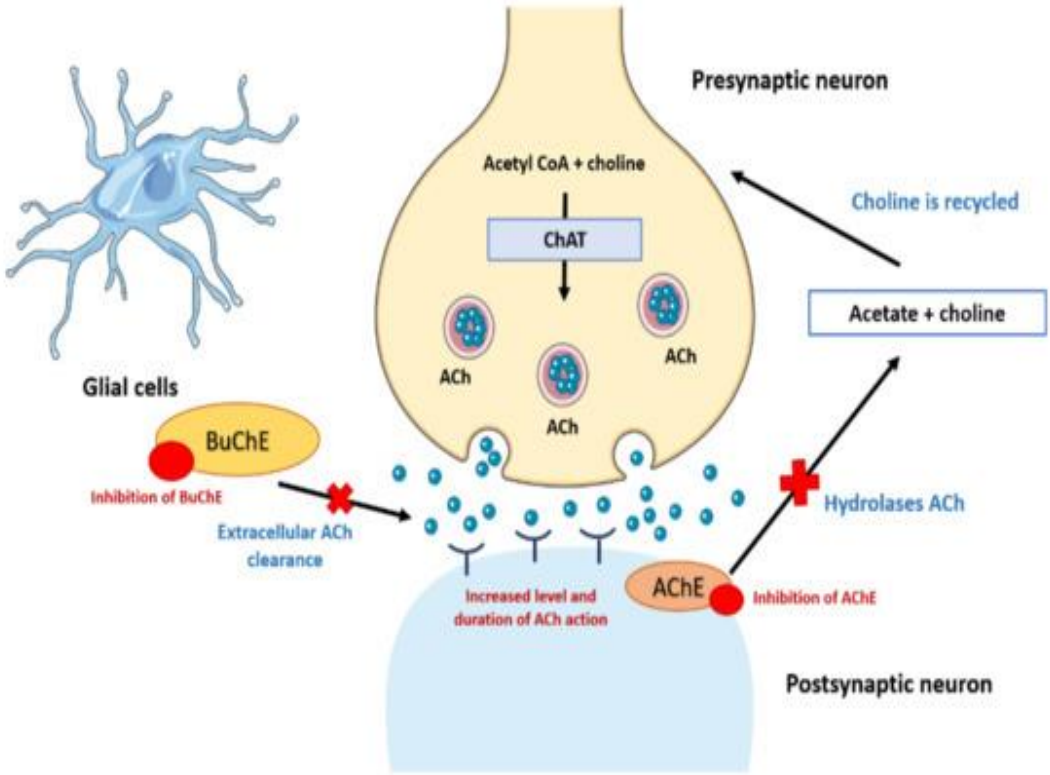

Figure 2.4 Mechanism of action of central AChE and BChE inhibitors according to the cholinergic hypothesis (Adopted from Lai et al., 2022).

2.4 Current treatment for AD

Even though Aβ and tau proteins are two of the most important disease targets in AD, clinical trials on several disease-modifying Aβ aggregation inhibitors, including tramiprosate (Alzhemed), colostrinin (O-CLN), scylloinositol (ELND005), 8-hydroxyquinoline (8-HQ), and PBT2, have been either less promising or unsuccessful. Hence, current treatment strategies for AD mainly rely on cholinesterase inhibitors to enhance central cholinergic neurotransmission and subsequently improve cognitive function in AD patients. However, the use of cholinesterase inhibitors is regarded as symptomatic treatment, in which this approach does not halt or reverse AD progression (Pope et al., 2005).

The FDA has approved four drugs to treat AD, three of which are cholinesterase inhibitors and one of which is an *N*-methyl-D-aspartate (NMDA) receptor noncompetitive antagonist (Zeng et al., 2021a). The first-generation cholinesterase inhibitor – tacrine (**6**), is discontinued for its use to treat AD due to its risk of causing hepatoxicity. Three cholinesterase inhibitors, donepezil (**7**), rivastigmine (**8**) and galantamine (**9**) are used to treat mild to moderate AD, whereas memantine (**10**), an NMDA antagonist, is used to treat moderate to severe AD (Colović et al., 2013; Zeng et al., 2021b; Lai et al., 2022). Memantine blocks the activation of NMDA receptors, lowering the excess release of glutamate (**11**), an excitatory neurotransmitter. Glutamate is produced in excess in the brain as AD progresses. The excessive quantities of glutamate then accumulate and activate the NMDA receptors, causing an excess of calcium to be released into the brain cells and causing neuronal damage (Johnson & Kotermanski, 2006). In recent years, a medication combination of donepezil and memantine - Namzaric® - has been developed to treat AD by targeting

two distinct pathways: central cholinergic and glutamate neurotransmission systems (McShane et al., 2019).

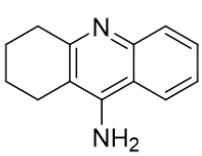

(**6**)

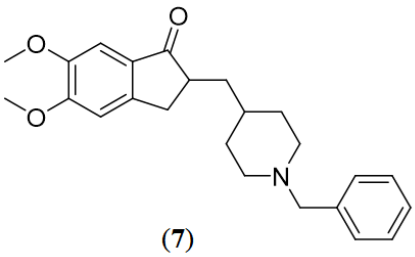

(**7**)

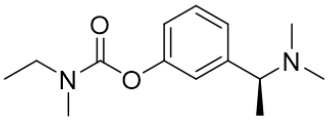

(**8**)

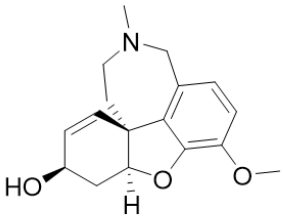

(**9**)

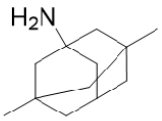

(**10**)

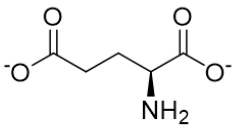

(**11**)

2.5 Plant alkaloids as lead compounds for treating Central Nervous System (CNS) diseases

Alkaloids are naturally occurring chemicals that contain one or more nitrogen atoms in addition to carbon, hydrogen, and, in most cases, oxygen as the basic structure (Hussain et al., 2018; Eguchi et al., 2019). The term "alkaloid" was introduced by Carl F. W. Meissner, a German chemist, in 1819. It is adapted from the Latin and Greek languages and means '*alkali-like*' (Croteau et al., 2000). According to the IUPAC Gold Book, alkaloids are basic compounds possessing nitrogen, often within a heterocyclic ring, as their structural unit. They are found primarily in plants but also include those of animal origins (IUPAC, 1997). However, nitrogen-containing primary metabolites, amino acids, peptides, proteins, nucleotides, nucleic acids, amino sugars, and antibiotics are not considered alkaloids (Pelletier, 1983).

Alkaloids are low-molecular-weight compounds (< 500 g/mol) that account for approximately 20% of secondary metabolites found in plants (Kaur & Arora, 2015). So far, over 12,000 alkaloids have been discovered in various plant genera (Kaur & Arora, 2015). Alkaloids are found primarily on higher plants, mainly flowering plant families from Rubiaceae, Annonaceae, Solanaceae, Rutaceae, Leguminoceae, Lauraceae, Loganiaceae, Amaryllidaceae, Papaveraceae, Apocynaceae etc. (Peng et al., 2019). Many CNS-targeted drugs and psychoactive substances are either derived from or structurally modified from plant alkaloids, for example, morphine (**12**), codeine (**13**), vincamine (**14**), atropine (**15**), cocaine (**16**), ephedrine (**17**), mescaline (**18**), levodopa (**19**), *N*, *N*-dimethyltryptamine (**20**), psilocin (**21**), and caffeine (**22**) (Bharate et al., 2018). The privileged alkaloid scaffolds among CNS drugs (**12**-**22**) and their sources of origin are summarized in Table 2.1.

Table 2.1 Privileged alkaloid scaffolds among CNS drugs

Structure	**Source of isolation or synthesis**	**Pharmacological activity**	**Reference**
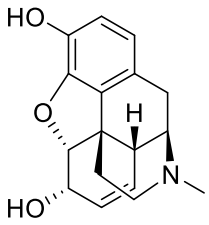 (**12**)	*Papaver somniferum* (Papaveraceae)	Opioid analgesic	Norn et al. (2005)
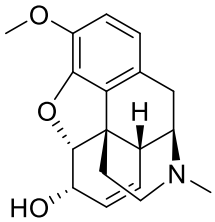 (**13**)	*Papaver somniferum* (Papaveraceae)	Opioid analgesic	Bhandari et al. (2011)

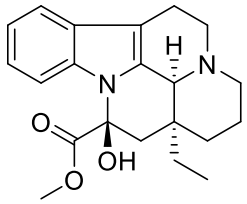 (**14**)	*Vinca major* (Apocynaceae)	Cognitive enhancer	Al-Rashed et al. (2021)
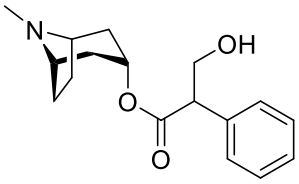 (**15**)	*Atropa belladonna, Datura stramonium, Datura metel*v (Solanaceae)	Antimuscarinic /Anticholinergic drug	O'Brien (1974)
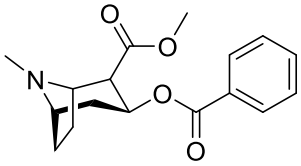 (**16**)	*Erythroxylum coca* (Erythroxylaceae)	CNS- stimulant	Pomara et al. (2012)
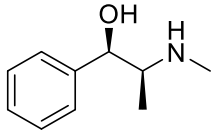 (**17**)	*Ephedra sinica* (Ephedraceae)	CNS-stimulant	Shorter & Segesser (2013)
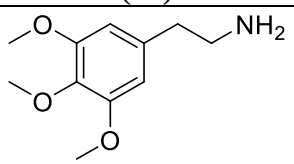 (**18**)	*Lophophora williamsii* (Cactaceae);	Hallucinogen, psychedelic	Cassels & Sáez-Briones (2018)
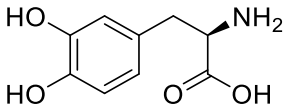 (**19**)	*Mucuna pruriens* (Fabaceae)	Anti-Parkinson's disease and dopamine-responsive dystonia	Bhattacharyya (2022)
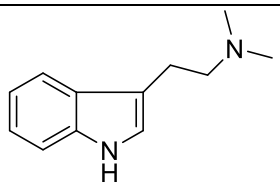 (**20**)	*Psychotria viridis* (Rubiaceae)	Hallucinogen, psychedelic	Cameroon & Olson (2018)
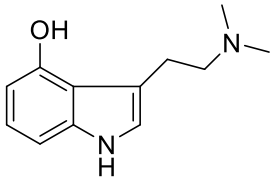 (**21**)	*Psilocybe baeocystis*	Psychedelic	Geiger et al. (2018)

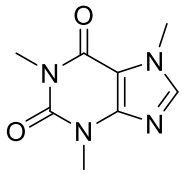 (**22**)	Coffee beans (*Coffea arabica*, *robusta* and *liberica*) (Rubiaceae)	CNS stimulant	Fredholm (2011)

Alkaloids are regarded as the most promising candidates for treating CNS disorders and neurodegenerative diseases (Lin et al., 2020). Because of their nitrogen-containing structure, alkaloids can efficiently interact with CNS receptors, transporters, and enzymes (Hussain et al., 2018). The nitrogen-containing structure (or the amine group) of alkaloids makes them basic in nature and enhances their active efflux at the blood-brain barrier (BBB). The amine functionality (positively charged) of alkaloids also promotes BBB permeability by interacting with the negatively charged groups of phospholipids at the BBB. As a result, alkaloids generally have higher BBB permeability than neutral or acidic compounds (Liu et al., 2004; Bharate et al., 2018). In addition, some plant alkaloids also possess a structural similarity to endogenous amine neurotransmitters, mimicking their activity at receptors and acting as receptor agonists. For example, mescaline (**18**) and levodopa (**19**) are structurally identical to dopamine (**23**) and noradrenaline (**24**), whereas *N*, *N*-dimethyltryptamine (**20**) and psilocin (**21**) contain a serotonin (**25**) skeleton in structure (Figure 2.5) (Heal et al., 2013).

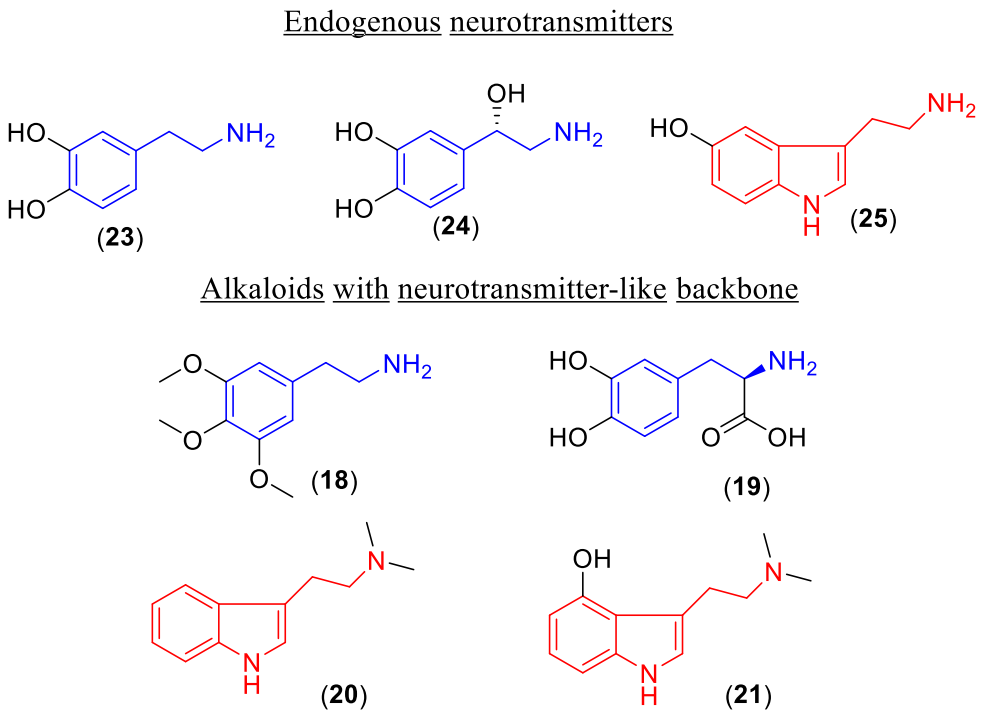

Figure 2.5 Structural similarity between neurotransmitters and alkaloid-derived CNS drugs

2.5.1 Classification of alkaloids

Alkaloids are nitrogen-containing plant metabolites that can be categorized according to their chemical structure, biochemical origins, taxonomical origin, and pharmacological action (Dey et al., 2020; Hussain et al., 2018; Amirkia & Heinrich, 2014).

2.5.1 (a) Biochemical origin

Hegnauer (1963) introduced the classification of alkaloids based on their biochemical precursors (amino acids) in the alkaloid biosynthesis pathway. According to Hegnauer's classification, alkaloids can be distinguished into three major types, which are (i) true alkaloids, (ii) proto alkaloids and (iii) pseudo-alkaloids. Their specific definitions are given below:

a) **True alkaloids** are derived from amino acids: L-ornithine, L-phenylalanine, L-tyrosine, L-histidine, L-arginine, L-tryptophan, and L-lysine, and they possess a nitrogen-containing heterocyclic ring. In plants, true alkaloids exist in three forms: (a) as a free base, (b) as *N*-oxide, or (c) as salt. True alkaloids readily form a water-soluble salt when conjugated with acid (Dewick, 2002; Aniszewski, 2007). Almost all true alkaloids are solid with a bitter taste. Examples of true alkaloids are morphine (**12**), atropine (**15**) and cocaine (**16**).

b) **Proto alkaloids** are amines that contain a nitrogen atom in the structure. Proto alkaloids are derived from an amino acid but do not form a heterocyclic ring system. L-tryptophan and L-tyrosine are the main biochemical precursors of proto-alkaloids. Mescaline (**18**), *N*, *N*-dimethyltryptamine (**20**), psilocin (**21**), and tryptophan-derived terpenoid indole alkaloids such as vincamine (**14**) are examples of proto-alkaloids (Chini et al., 1992; Lichman, 2020).

c) **Pseudo-alkaloids** are not derived from amino acids. However, they have a nitrogen-containing heterocyclic ring, in which the nitrogen is usually introduced late in the biosynthesis process through an enzymatic reaction such as transamination. The biochemical precursors of pseudo-alkaloids are geraniol, acetate, ferulic acid, adenine, or guanine (Casciaro et al., 2020). Purine-like alkaloids such as caffeine (**22**) are the most common pseudo-alkaloids.

2.5.1 (b) Chemical structure

Alkaloids can be easily distinguished based on their chemical structure. It is the most common and widely accepted method for classifying alkaloids, with the existence of a basic heterocyclic nucleus serving as the primary criterion (Dey et al., 2020).

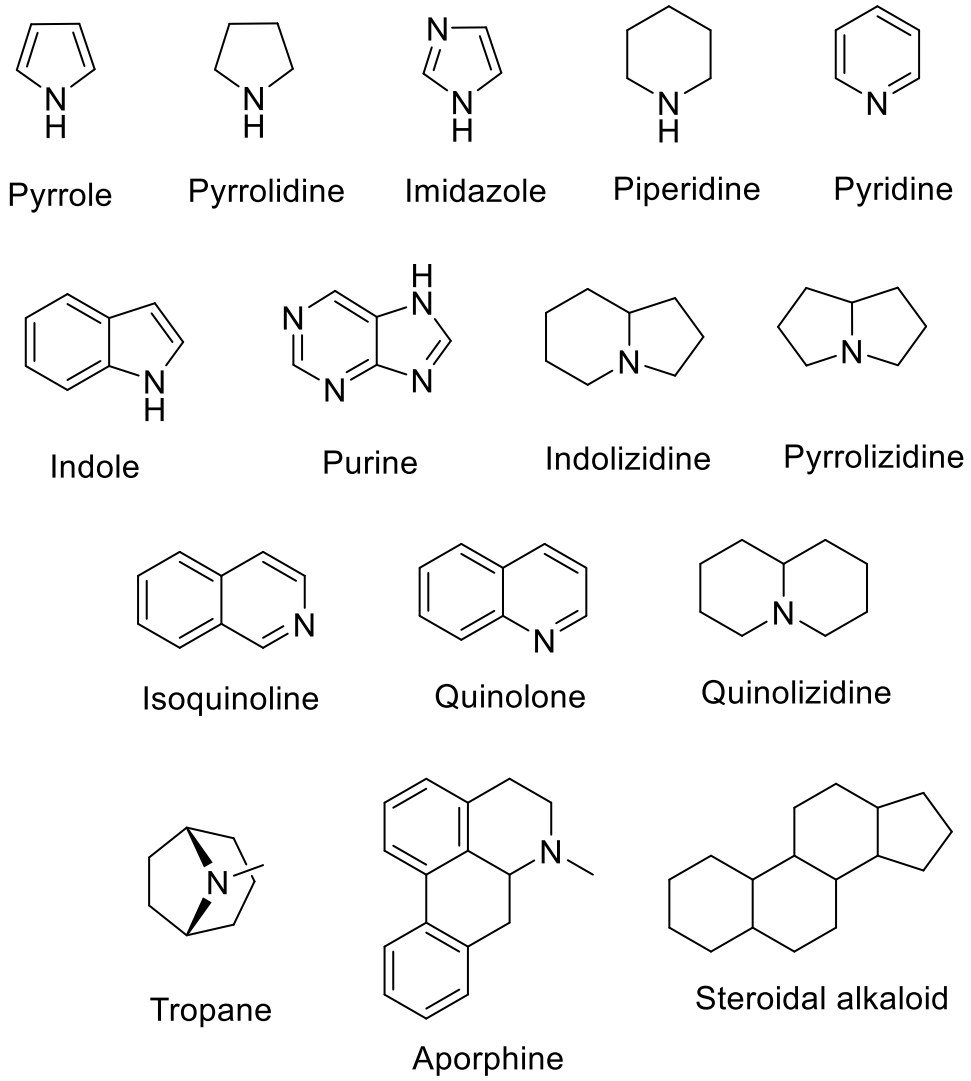

Figure 2.6 Structural classes of alkaloids based on their ring structure.

Heterocyclic alkaloids, including all true alkaloids with some exceptional proto- and pseudo-alkaloids, are further divided into 15 subclasses: indole, isoquinoline, pyrrolizidine, pyrrolidine, quinolizidine, tropane, purine, piperidine, aporphine, quinolone, imidazole, pyrrole, indolizidine, pyridine and steroidal alkaloids according to their backbones (Figure 2.6) (Casciaro et al., 2020). For example, morphine (**12**) and codeine (**13**) are classified as isoquinoline alkaloids, while caffeine (**22**) is known as a purine alkaloid.